1

Optical configurations

1.1 Introduction

▷ *In this section we show that for the purpose of the rest of these notes, the effect of a gravitational wave is to change the measured distance between to free masses by a fractional amount $h/2$ where h is the gravitational wave strain amplitude.*

Gravitational waves (GW) are perturbations in the space-time metric [1]. Entering into details of how they are generated or how they propagate is beyond the scope of these notes. Then interested reader should refer to any one fo the many good books on General Relativity [2], and gravitational wave theory [3]. In a otherwise flat space-time, the metric perturbation can be written as

$$g_{\mu\nu} = \eta_{\mu\nu} + h_{\mu\nu} \tag{1.1}$$

where η is the flat background Minkowski metric, and h is the components due to the gravitational waves. In general, far from the source, gravitational waves are very weak, i.e. $|h_{\mu\nu}| \ll 1$. It can be shown from the equation of General Relativity (GR) that there are only two possible polarizations for propagating GWs. Using the connection that $\mu, \nu = 0$ indicates the time coordinate, and considering a plane GW with frequency f propagating along the z axis, the metric perturbation can be written as the same of two components:

$$h_{\mu\nu}(z,t) = \exp\left[2i\pi f\left(t - \frac{z}{c}\right)\right] \cdot \left(h_+ \epsilon^{(+)}_{\mu\nu} + h_x \epsilon^{(\times)}_{\mu\nu}\right) \tag{1.2}$$

where the two polarizations base tensors have been denoted with $\epsilon^{(i)}_{\mu\nu}$:

$$\epsilon^{(+)} = \begin{pmatrix} 0 & 0 & 0 & 0 \\ 0 & 1 & 0 & 0 \\ 0 & 0 & -1 & 0 \\ 0 & 0 & 0 & 0 \end{pmatrix} \qquad \epsilon^{(\times)} = \begin{pmatrix} 0 & 0 & 0 & 0 \\ 0 & 0 & 1 & 0 \\ 0 & 1 & 0 & 0 \\ 0 & 0 & 0 & 0 \end{pmatrix} \tag{1.3}$$

[1] Albert Einstein. Über Gravitationswellen. *Sitzungsberichte der Königlich Preussischen Akademie der Wissenschaften Berlin*, pages 154–167, 1918

[2] C. W. Misner, K. S. Thorne, and J. A. Wheeler. *Gravitation*. W.H. Freeman and Co., 1973; and Robert M Wald. *General relativity*. Chicago Univ. Press, Chicago, IL, 1984

[3] P. R. Saulson. *Fundamentals of Interferometric Gravitational Wave Detectors*. World Scientific Publishing Co, 1994. DOI: 10.1142/2410

It is common to say that the effect of gravitational waves is to change the distance between free falling masses. To be concrete, let us consider the thought experiment of measuring the distance between two masses separated by a macroscopical distance L, and not subject to any external force. Experimentally, one way to measure the distance would be to send a light pulse from the first mass to the second, have it reflected back, and measure the time of arrival at the first mass. In absence of any GW, the measured time is

$$\Delta t = \frac{2L}{c} \tag{1.4}$$

where c is obviously the speed of light in vacuum (and we clearly assume the light propagation to happen in vacuum). What happens when a GW as the one considered above impinges on this system? The light propagation is described locally, at each point along the path, by

$$0 = ds^2 = g_{\mu\nu}dx^\mu dx^\nu = (\eta_{\mu\nu} + h_{\mu\nu})dx^\mu dx^\nu \tag{1.5}$$

For simplicity, let us assume that the GW is propagating along the z direction and that the two masses are separated along the x direction, which means that the light propagation is along the x axis. Only the 11 component of $h_{\mu\nu}$ matters, so by denoting $h = h_+\epsilon_{11}^{(+)} + h_\times\epsilon_{11}^{(\times)}$ we have:

$$0 = -c^2dt^2 + (1 + h(t,x))\,dx^2 \tag{1.6}$$

where $h(t,x)$ is the GW amplitude at time t and at the position x of the light pulse we are following. We can compute the infinitesimal travel time dt from the equation above and integrate it along the entire propagation distance. Assuming the light pulse to be emitted at time $t = 0$ and considering for the moment being only the outbound propagation, we have

$$t' = \int_0^{t'} dt = \frac{1}{c}\int_0^L \sqrt{1 + h(t,x)}dx \tag{1.7}$$

where again we stress that the GW amplitude $h(t,x)$ has to be evaluated at the position where the light pulse is at time t. In general this is a very complicate caution to solve, since x is a function of t through the dilation and compression effect of the GW. Fortunately (from a theoretical point of view, unfortunately from an experimental perspective) GWs are very weak, meaning that $|h| \ll 1$. This simplifies the previous equation greatly. First of all, we can expand the square root at first order. Secondly, we can take $t = x/c$, since any more terms linear in h would contribute to the integral at the second order. Therefore we have

$$t' = \frac{L}{c} + \frac{1}{2c}\int_0^L h\left(\frac{x}{c}\right)\,dx = \frac{L}{c} + \frac{1}{2c}\int_0^L h_0 \exp\left(2i\pi f\frac{x}{c}\right)\,dx \tag{1.8}$$

which is easily computed to yield:

$$t' = \frac{L}{c} + \frac{h}{4\pi i f}\left[\exp\left(\frac{2i\pi f L}{c}\right) - 1\right] \tag{1.9}$$

It is straightforward to repeat the computation for the light pulse reflected back, considering that now $t = (2L - x)/c$. Summing the two travel times and subtracting the value in absence of GWs, we get finally

$$\Delta t' - \Delta t = h\frac{2L}{c}\exp\left(i\pi f\frac{2L}{c}\right)\operatorname{sinc}\left(\pi f\frac{2L}{c}\right) \tag{1.10}$$

T . We see that the effect of the GW is simply to modify the round trip travel time with a term which is directly proportional to wave amplitude, plus a frequency dependent term. This term can be understood considering that for GW of high frequency, the light pulse travel time can be larger than GW period, thus effectively averaging over multiple oscillations and reducing the resultant effect. For GW frequencies $f \ll c/L$ this frequency dependent term is not relevant and equal to one. To be concrete, for a travel length of $L = 4$km the response drops by a factor of $\sqrt{2}$ with respect to the response at zero frequency when $f \simeq 16.7$kHz. This is often called the bandwidth of the response. Therefore, for GWs in the audio range, i.e. up to a few kilohertz, we can neglect this frequency dependence.

Here we define $\operatorname{sinc}(x) = \sin x/x$

The reader can refer to the jupyter notebook `chapter_1_1_ResponseToGW` to see an example computation of the frequency response described here.

An equivalent way to express eq. 1.10 is to consider the effect of a GW as a change in the measured distance between the two free falling masses

$$\delta L_{GW} = h\,L\exp\left(i\pi f\frac{2L}{c}\right)\operatorname{sinc}\left(\pi f\frac{2L}{c}\right) \tag{1.11}$$

which, for low GW frequencies, simplifies to

$$\delta L_{GW} = h\,L \tag{1.12}$$

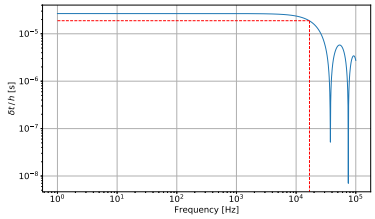

Figure 1.1: Time dilation induced by a GW for the propagation of a light pulse over 4 km, as a function of the GW frequency.

Therefore, for the rest of these notes, we will simply consider eq. 1.12 as the correct description of the effect of a GW on our detector system.

One last note before moving forward: the differential nature of the metric perturbation in eq. 1.3 shows that the change in distance in two orthogonal direction has different sign or amplitude. Indeed, for a GW propagating along the z direction, and polarized in the $+$ direction, aligned with the x and y axis, the distance fluctuations have the same amplitude along x and y, but opposite sign. For other directions of propagation, or mixtures of the polarizations, the relation is more complex. Nevertheless, the differential nature of GWs will play a key role in the technique used for their detection.

1.2 *Lasers, mirrors and detectors*

▷ A GW of astrophysical origin, with an amplitude of the order of 10^{-21}, would produce an effective change in distance of about 4×10^{-18} m over a baseline of 4 km. How can we detect such a small change in distance? The first gravitational wave detectors were resonant bars, but since the late '90s the most sensitive detectors are based on laser interferometers. So this section will introduce the basic concepts needed to describe laser beams and mirrors.

Lasers

Modern interferometer use lasers as light sources. The physics of how light is generated inside a laser is very interesting and complex, but beyond the scope of this presentation. For now, we can assume that a laser is a perfect monochromatic source of light, with a wavelength λ and frequency f. Light can be described classically in terms of plane waves that have to obey the Maxwell's equations. The electric and magnetic field at each position in space and time must obey the wave equation derived from Maxwell's equations [4]. In the most general case a plane wave can have two polarization components, however most laser source have a definite linear polarization. Therefore we can simplify our description of the laser field and use a scalar number, which is proportional to the electric field amplitude:

Laser beams are clearly not plane waves. We shall see later in these notes that the most precise way to describe them is in terms of Gaussian beams. However, the description provided here is enough to understand most of the physics of gravitational waved interferometric detectors.

[4] J. D. Jackson. *Classical Electrodynamics, 3rd Edition*. Wiley-VCH, July 1998

$$E(\mathbf{x}, t) = Ee^{i\mathbf{k}\cdot\mathbf{x} - i\omega t} \tag{1.13}$$

where $\mathbf{x}$ is the spatial coordinate, t the time, $\mathbf{k}$ and ω are the wavevector and angular frequency of the wave, defined by

In equation 1.13 above we use the customary complex exponential for the oscillating part of wave. In this notation, the electric field amplitude E can also be complex. The amplitude of this complex number describes the physical peak amplitude of the field, and the argument of the complex number the phase at a reference position in space. The complex notation must be understood as follows: the physical electric field, which must be real, is given at any position and time, by the real part of $E(\mathbf{x}, t)$.

$$\omega = 2\pi f \tag{1.14}$$

$$\mathbf{k} = \frac{2\pi}{\lambda}\mathbf{n} \tag{1.15}$$

where $\mathbf{n}$ is the direction of propagation. Typical lasers used in GW detectors have a wavelength of 1064 nm, corresponding to a frequency of about 280 THz.

In the following we will neglect the time oscillating phase, since it is typically too fast to be detected. However, eq. 1.13 shows that when propagating over a distance L, a plane wave accumulates an additional phase kL. This is at the base of out idea of using plane waves to detect gravitational waves. Instead of monitoring the time of arrival of light pulse, as we did in the previous section, we continuously measure the phase of light waves. In some sense, this is equivalent to measuring the time of arrival of the wave maxima, but it can be very precise since we can average multiple maxima, and there are a lot of them in a laser beam , even in very short period of time.

The phase accumulated in propagation varies very rapidly with the distance: $\phi = kL = 2\pi\frac{L}{\lambda}$. Therefore every wavelength the phase gets a full 2π, which brings the field back to the original value. For this reason, in most cases the macroscopic length does not matter for the propagation phase. Only the microscopic component, i.e. the fractional part that goes from the closest multiple of the wavelength to the actual distance, matters for the phase of the field. Therefore we often decompose any length L in a macroscopic length which is an integer multiple of a wavelength $L_{macro} = N\lambda, N \in \mathbb{N}$, and a microscopic length L_{micro} that is typically smaller than a wavelength $|L_{micro}| \lesssim \lambda$

Detectors

The power transported by the plane wave can be computed using the Poynting vector[5]. In the simple description in terms of a scalar used above, the power averaged over an oscillation cycle is proportional to the square of the absolute value of the field E. To keep the notation simple, we make the assumption that the field E is rescaled such that the power transmitted through a surface perpendicular to the direction of propagation is simply

$$P(\mathbf{x}) = |E(\mathbf{x}, t)|^2 \tag{1.16}$$

This is independent of time, since the absolute value gets rid of the oscillating term.

[5] J. D. Jackson. *Classical Electrodynamics, 3rd Edition*. Wiley-VCH, July 1998

Having covered the sources, let's now focus on the detection part, or in other words how to convert properties of a laser beam into electrical signals that cane measured on a oscilloscope or digitized and used in our computers. The most common detector used in most optics experiment is the *photodiode*: a semiconductor slab that converts the light impinging into the surface in electrons via photoelectric effect [6]. The number of photoelectrons is proportional to the number of incident photons, the ratio being often called the quantum efficiency η of the detector. The photodiode produces an output current which is directly proportional to the number of photons:

[6] Albert Einstein. Concerning an heuristic point of view toward the emission and transformation of light. *Annalen Phys.*, 17:132–148, 1905

$$I = \eta q_e \frac{P}{\hbar\omega} \tag{1.17}$$

where q_e is the electron charge and $\hbar$ is the reduced Planck's constant. This current can be converted into an electric signal by the appropriate trans-impedance electronic circuit and provide a measurement of the power carried by the laser beam.

One very important note here is that using a photodiode, we have no access to the rapidly fluctuating phase of the field, but only to the averaged power. However, if we have two field impinging on the same photodiode, and interfering, the relative phase between the two is accessible. Indeed we have

$$P = |E_1 + E_2|^2 = |E_1|^2 + |E_2|^2 + 2\Re\left(E_1^* E_2\right) \quad (1.18)$$
$$= |E_1|^2 + |E_2|^2 + |E_1| \cdot |E_2| \cos\phi_{12} \quad (1.19)$$

where $\Re(\cdot)$ denotes the real part and ϕ_{12} is the relative phase of the two fields.

Mirrors

The final ingredient to build an interferometer is a mirror. Astronomical telescopes (and bathroom mirrors by the way) use a thin layer of metal to reflect light. This provides a broadband (wavelength independent) reflection, but the efficiency is not very high: typical aluminum coatings reflects of the order of 90% of the incident power. Silver and gold coatings can give reflection coefficients as high as 95-99%. This is however not sufficient for GW application, where a reflectivity of more than 99.999% are needed. For this reason, dielectric coatings are used. They are composed of multiple alternating layers of dielectric materials with different refractive indexes. Fresnel reflection at each interface [7] creates multiple returning waves, and the interference between those wave can be fine tuned by changing the thickness of each layer, to provide the desired high reflectivity[8].

[7] See for example WikiPedia `https://en.wikipedia.org/wiki/Fresnel_equations`

[8] S. J. Orfanidis. *Electromagnetic Waves and Antennas*. http://eceweb1.rutgers.edu/ orfanidi/ewa/, 2016

Regardless of the way the mirror is actually built, it can be simply described in terms of an amplitude reflection and transmission coefficient, r and t respectively, such that the field reflected and transmitted are given by (see also fig. 1.2):

$$E_r = rE_i \quad (1.20)$$
$$E_t = tE_i \quad (1.21)$$

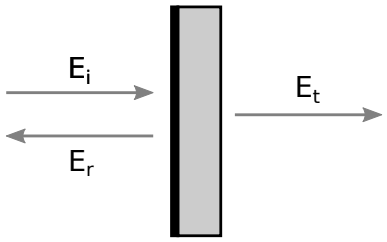

Figure 1.2: Fields reflected and transmitted by a simple mirror.

The transmission and reflection coefficient can in general be complex, since the phase can depend on the details of the coating, through the Fresnel equations. However, remember that the absolute phase of the field at any given point is not physically accessible with any measurement, while only the relative phase between fields is important. Therefore we have some freedom to define the phase of the reflection and transmission coefficients, provided we do not violate energy conservation. The first requirement is that the total ingoing energy must

be equal to the total outgoing energy, minus the power which is loss on the mirror because of absorption or scattering:

$$|r|^2 + |t|^2 + \mathcal{L} = 1 \tag{1.22}$$

where $\mathcal{L}$ is the fractional power loss in the mirror. A more stringent requirement is obtained considering field ingoing from both sides of the mirror, see fig. 1.3:

$$|E_2|^2 + |E_4|^2 = (1 - \mathcal{L}) \left(|E_1|^2 + |E_3|^2 \right) \tag{1.23}$$

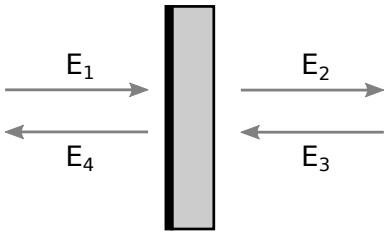

Figure 1.3: Fields reflected and transmitted by a simple mirror, with sources on both sides.

The outgoing fields can be written in terms of the ingoing fields and the reflection and transmission coefficients, which can have different phases for beam coming from the right or from the left of the mirror (but they have the same absolute values):

$$E_4 = r_L E_1 + t_L E_3 \tag{1.24}$$
$$E_2 = r_R E_3 + t_R E_1 \tag{1.25}$$

using those last two equations in eq. 1.23 and enforcing the constraint in eq. 1.22 yield the following additional identity that must be satisfied for our choice of the coefficients:

$$r_R^* t_R + r_L t_L^* = 0 \tag{1.26}$$

This equation can be satisfied in many ways. Here we use the convention that $t_R = t_L$ and $r_R = -r_L = r$, where we assume that the reflection coefficient is positive for the beam impinging on the main side of the mirror, and negative for the beam impinging from the back side.

Another alternative convention is to have $t_R = t_L$ and $r_R = r_L$. Then either the reflection or the transmission coefficients must be imaginary. For example $r_L = r_R = ir$ and $t_L = t_R = t$ where r and t are now the (real) amplitude reflection and transmission coefficients.

In summary, a mirror is described by two real coefficients r and t which determine the amplitude of the reflected and transmitted fields respectively, such that:

$$E_r = \pm r E_i \tag{1.27}$$
$$E_t = t E_i \tag{1.28}$$

The power reflection and transmission coefficients are clearly given by $\mathcal{R} = r^2$ and $\mathcal{T} = t^2$.

1.3 *Michelson interferometer*

▷ Now we have all the components to construct the basic version of the instrument that we use to detect gravitational waves. The idea is to build an optical system that can convert (transduce) gravitational waves to variation of an optical field power or phase, that can then be detected using suitable ensemble of photodiodes.

It is interesting that the basic idea dates back to the very first Michelson and Morley experiment[9], probably one of the most famous "failed" experiment, since it was devised to prove the existence of ether, but did not find any. This negative result is among the reasons that triggered the development of the Theory of Special Relativity [10].

[9] A. A. Michelson and E. W. Morley. On the relative motion of the Earth and the luminiferous ether. *American Journal of Science*, 34:333–345, November 1887. DOI: 10.2475/ajs.s3-34.203.333

[10] A. Einstein. Zur Elektrodynamik bewegter Körper. *Annalen der Physik*, 322:891–921, 1905. DOI: 10.1002/andp.19053221004

Interference

Figure 1.4 shows a scheme of a simple Michelson interferometer. A laser beam is split in half by a semi-reflective mirror (called the *beam splitter*). The two resulting beams then travel along two orthogonal arms with roughly equal length, are reflected by high reflectivity mirrors, recombine at the beam splitter where they interfere. The resulting beam at the *anti-symmetric port* is finally detected by a photodiode.

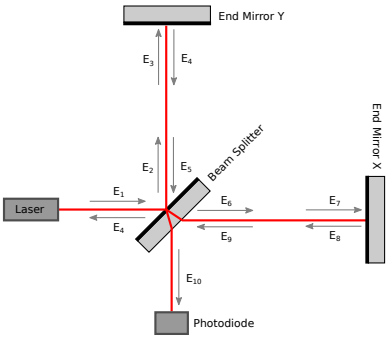

Figure 1.4: A Michelson interferometer, with the definition of the fields.

The basic idea is that a GW incident on the detector will cause a change in the distance between the beam splitter and the two end mirrors. The amount of change in each arm depends on the wave direction of propagation and polarization. In the optimal case, when the GW is propagating perpendicularly to the detector plane (the z axis) and it is in a $+$ polarization aligned with the two arms, the change in distance is $\delta L^{(h)}_{X,Y} = \pm L_{X,Y} h$ where L is the macroscopic length of the arms and h as usual the GW amplitude.

Figure 1.4 lists all the relevant fields. In this first example we will write explicitly the equations that connects the fields together, due to propagation or reflection. First of all, assuming the beam splitter to be perfectly balanced (having a reflectivity of exactly 50% in power, meaning $1/\sqrt{2}$ in amplitude) allows us to write the fields entering the two interferometer arms:

$$E_2 = \frac{i}{\sqrt{2}} E_1 \tag{1.29}$$

$$E_6 = \frac{1}{\sqrt{2}} E_1 \tag{1.30}$$

where few used our convention for the imaginary reflection and real transmission. Those two fields then propagate to the end mirrors, acquiring a phase related to the arm lengths L_X and L_Y

$$E_3 = e^{ikL_Y} E_2 \tag{1.31}$$

$$E_7 = e^{ikL_Y} E_6 \tag{1.32}$$

Then the fields are reflected by the end mirrors (in both cases from

the main side):

$$E_4 = r_Y E_3 \tag{1.33}$$
$$E_8 = r_X E_7 \tag{1.34}$$

and propagate back to the beam splitter

$$E_5 = e^{ikL_Y} E_4 \tag{1.35}$$
$$E_9 = e^{ikL_X} E_8 \tag{1.36}$$

where they interfere to create the beam that will be detected

$$E_{10} = -\frac{1}{\sqrt{2}} E_9 + \frac{1}{\sqrt{2}} E_5 \tag{1.37}$$

where the minus sign is due to the reflection from the back side of the beam splitter. A bit of algebra allow us to put all the previous equations together and compute directly the anti-symmetric port file E_{10} as a function of the input and the other interferometer parameters:

$$E_A = E_{10} = -\frac{1}{2}\left[e^{2ikL_X} r_X - e^{2ikL_Y} r_Y\right] E_1 \tag{1.38}$$

In a similar way we can trace the field that returns toward the laser at the *symmetric* or *reflection port*:

$$E_S = E_4 = \frac{1}{2}\left[e^{2ikL_X} r_X + e^{2ikL_Y} r_Y\right] E_1 \tag{1.39}$$

If we define the average arm length $L = \frac{L_X + L_Y}{2}$ and the length difference $\Delta L = L_X - L_Y$ then we can write:

$$E_A = -\frac{1}{2} e^{2ikL}\left[e^{ik\Delta L} r_X - e^{-ik\Delta L} r_Y\right] E_1 \tag{1.40}$$
$$E_S = +\frac{1}{2} e^{2ikL}\left[e^{ik\Delta L} r_X + e^{-ik\Delta L} r_Y\right] E_1 \tag{1.41}$$

What will the photodiode at the anti-symmetric port detect? To answer this question we can simply compute the squared absolute value of the field E_A, which yields

$$P_A = \frac{P_i}{4}\left[r_X^2 + r_Y^2 - 2 r_X r_Y \cos 2k\Delta L\right] \tag{1.42}$$

In similar way, if we place a photodiode at the symmetric port, we detect a power:

$$P_S = \frac{P_i}{4}\left[r_X^2 + r_Y^2 + 2 r_X r_Y \cos 2k\Delta L\right] \tag{1.43}$$

The anti-symmetric and symmetric powers compute above show the typical behavior of interference fringes: the signal detected by a

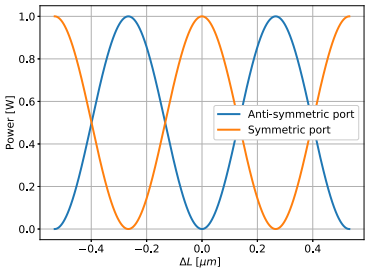

Figure 1.5: Power measured by the two photodiodes in a Michelson interferometer, as a function of the arm length difference tuning.

One might wonder how we can place a photodiode at the symmetric port, without blocking the input laser. One way could be to place a beam splitter with a small reflectivity, to pick off part of the beam. A more common approach is to use a Faraday isolator: a device that allow light to propagate only in one direction, reflecting the light coming from the wrong direction to an auxiliary port.
The reader can refer to the jupyter notebook `chapter_1_3_MichelsonIFO` to see examples of computations for a Michelson interferometer.

photodiode changes as a function of the length difference between the two interferometer arms, in a way which is periodic, with period $\lambda/2$. Moreover, the power detected at either of the two ports does not depend on the average arm length L, but only on the difference ΔL. Let us focus on the argument of the oscillatory component for the moment being, and expand it as follows:

$$2k\Delta L = 2\frac{\omega_0 + \delta\omega}{c}(\Delta L_0 + \delta L) \tag{1.44}$$

Here we introduced a few new terms:

- $\omega_0 = 2\pi f_L$ is the nominal angular frequency of the laser, typically of the order of 280 $\times 10^{12}$ Hz.
- $\delta\omega$ is a "small" fluctuation of the laser frequency around the nominal value. Even very good laser source have line widths of the order of kHz or larger.
- ΔL_0 is a macroscopic length difference. By macroscopic we mean that $\Delta L \gg \lambda$. We can always assume that ΔL_0 is an integer multiple of half wavelength, so that $2k\Delta L_0$ is always a multiple of 2π and does not contribute to the oscillatory part of the power.
- δL contains the microscopic contribution to the length difference, and it is of the order of the wavelength or smaller. This δL comes from the static tuning of the length difference that we do to enforce a particular resonance condition, and from residual motion of the mirrors. Also, it contains a (very) small contribution from gravitational wave signals.

If we expand eq. 1.44 we have

$$2k\Delta L = 2\frac{\omega_0}{c}\Delta L_0 + 2\frac{\omega_0}{c}\delta L + 2\frac{\Delta L_0}{c}\delta\omega + 2\frac{\delta\omega\delta L}{c} \tag{1.45}$$

The first term can be ignored, since by construction it is a multiple of 2π. The last term is negligible with respect to the others, since it is second order in small quantities: $\delta\omega \simeq 10^4$ rad/s and $\delta L \simeq 10^{-6}$ m.

As shown in fig. 1.5 the choice of $\Delta L = 0$ makes the power at the anti-symmetric port minimum. This is usually called the *dark fringe condition*, in contrast to the *bright fringe condition* that corresponds to the maximum power at the anti-symmetric port. If the reflectivity of the two end mirrors is equal, as is the case for the curves shown in fig. 1.5, then the minimum power is exactly zero. If the mirror reflection coefficients are different, then the minimum power is no more zero. Figure 1.6 shows what happens when $r_X = 0.95$ and $r_Y = 0.65$. First of all, the maximum power at either port is no more equal to the input power, since some light is lost in transmission of

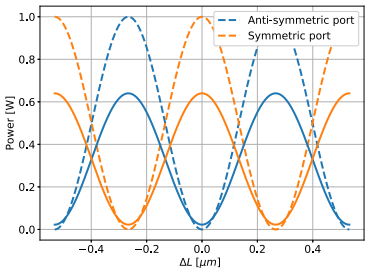

Figure 1.6: Power measured by the two photodiodes in a Michelson interferometer, as a function of the arm length difference tuning. The dashed curves are computed for balanced mirror reflectivity $r_X = r_Y = 1$. The solid curves instead are computed for $r_X = 0.95$ and $r_Y = 0.65$.

the end mirrors. Moreover, the minimum power when at the dark fringe condition is no more zero. This residual power is due to the imperfect destructive interference that is caused by the imbalanced power coming back from the arms. The *contrast defect* of the Michelson interferometer is defined as the ratio of the minimum power at the anti-symmetric port divided by the maximum power at the anti-symmetric port:

$$C = \frac{r_X^2 + r_Y^2 - 2r_X r_Y}{r_X^2 + r_Y^2 + 2r_X r_Y} = \left(\frac{r_X - r_Y}{r_X + r_Y}\right)^2 \tag{1.46}$$

Optical gain

So far we have not answered the main question, that is: how can we use a Michelson interferometer to detect gravitational waves? Toward this goal, let us assume that a monochromatic GW with amplitude h_0 and angular frequency ω_{GW} is incident on a Michelson interferometer, so to create an equivalent distance change between the beam splitter and two end mirrors. This change in distance is differential, because of the polarization nature of the GW. In other words, the X and Y arm lengths are modulated in time as follows

$$L_X(t) = L + Lh_0 \sin \omega_{GW} t \tag{1.47}$$
$$L_Y(t) = L - Lh_0 \sin \omega_{GW} t \tag{1.48}$$

where $h_0 \ll 1$ and also $|\delta L| \ll \lambda$. We can compute the response of the Michelson interferometer to the GW by using $\delta L(t) = L_X(t) - L_Y(t) = \delta L_0 + 2Lh(t)$, where δL_0 is the static tuning of the Michelson interferometer that sets the working position in the resonance fringe. Expanding eq. 1.42 at first order in h we get:

$$P_A(t) = P_{A,0}(\delta L_0) + G(\delta L_0) \cdot h(t) \tag{1.49}$$
$$P_{A,0}(\delta L_0) = \frac{P_i}{4}\left[r_X^2 + r_Y^2 - 2r_x r_Y \cos 2k\delta L_0\right] \tag{1.50}$$
$$G(\delta L_0) = \frac{4\pi L}{\lambda} r_X r_Y P_i \sin 2k\delta L_0 \tag{1.51}$$

where we have defined the static power at the anti-symmetric port $P_{A,0}$ and the *optical gain* G of the Michelson interferometer, which are both functions of the tuning δL_0.

Shot noise

Naively, one would expect that the best condition to detect gravitational waves is the one that provides the target optical gain. This

corresponds to the position where the slope of the power at the anti-symmetric port with respect to length change is the largest. Clearly, this corresponds to the *half fringe* condition, i.e. the Michelson interferometer tuning that make the power half way between the minimum and the maximum values. In the real world, our ability to measure small power fluctuations with any detector is limited by technical and fundamental noise sources, that produce spurious changes in the power, indistinguishable from what is caused by the GW signal. The lowest power fluctuations we can detect on a laser beam is limited by the quantum nature of light. This quantum noise limit can be computed from first principles using quantum electrodynamics, but for a simple configuration like our Michelson interferometer we can derive the correct result by simple arguments.

The reader will find a more detailed quantum treatment of this topic in later chapter.

When we measure the power impinging on a photodiode we are making a photon counting experiment, since the photocurrent is proportional to the number of photons that hit the detector per unit time. Since the arrival time of the photons are uncorrelated, the number of detections during any amount of time follow a Poisson statistics, where the probability of detecting any given number of photons in an interval Δt is given by

$$\mathrm{Prob}(n) = e^{-m}\frac{m^n}{n!} \tag{1.52}$$

where m is the only parameter of the distribution and it is related to the average number of photons detected in the time interval Δt:

$$m = \mathcal{E}[n] = \frac{P\Delta t}{\hbar\omega} \tag{1.53}$$

where $\mathcal{E}[\cdot]$ denotes the expectation of the argument. A basic property of the Poisson distribution is that its variance is equal to the mean, so that $\mathcal{E}[(n-\bar{n})^2] = \mathcal{E}[n]$, where we denoted the expectation of n as $\bar{n} = \mathcal{E}[n]$ for the sake of brevity. This allows us to compute the variance in the detected power

$$\mathcal{E}[(P-\bar{P})^2\Delta t^2] = (\hbar\omega)^2\mathcal{E}[(n-\bar{n})^2] = (\hbar\omega)^2\mathcal{E}[n] = \hbar\omega\bar{P}\Delta t \tag{1.54}$$

The numbers of photons detected during distinct time periods are uncorrelated, therefore

$$\begin{aligned}\mathcal{E}[(P(t_1)-\bar{P})(P(t_2)-\bar{P})\Delta t^2] &= \mathcal{E}[(P-\bar{P})^2\Delta t^2]\delta(t_1-t_2)\\ &= \hbar\omega\bar{P}\Delta t\delta(t_1-t_2)\end{aligned} \tag{1.55}$$

This allows us to compute the *shot noise* as the spectral density of the power measurement.

The reader who is not familiar with spectral densities can refer to the integration box below.

$$S_P(\Omega) = \lim_{T\to\infty}\frac{2}{T}\mathcal{E}\left[\left|\int_{-T}^{T}(P(t)-\bar{P})e^{-i\Omega t}\,dt\right|^2\right] \tag{1.56}$$

where the factor 2 comes from out desire to use single sided spectral densities. A bit of manipulation allows us to get the result we seek

$$\begin{aligned} S_P(\Omega) &= \lim_{T\to\infty} \frac{2}{T}\int_{-T}^{T}\int_{-T}^{T} \mathcal{E}[(P(t_1)-\bar{P})dt_1(P(t_2)-\bar{P})dt_2]e^{-i\Omega(t_1-t_2)} \\ &= \lim_{T\to\infty} \frac{2}{T}\int_{-T}^{T} \hbar\omega\bar{P}dt_1 = 2\hbar\omega\bar{P} \end{aligned} \tag{1.57}$$

We have found that the quantum nature of light imposes a limit to the accuracy we can achieve when measuring a laser beam with an average power P, described by a white shot noise that has an amplitude spectra density proportional to the square root of the power:

$$S_P^{1/2}(\Omega) = \sqrt{2\hbar\omega\bar{P}} \tag{1.58}$$

Therefore, to decide what is the value of the Michelson interferometer tuning that gives us the best chance to detect a GW signal, we have to compare the power fluctuation generated by the GW with the shot noise, and maximize the *signal to noise ratio* (SNR).

Spectral densities

Consider a signal $x(t)$, i.e. the result of a physical measurement that varies over time. The notation $x(t)$ suggest that x is a continuous function of time, while in most cases real measurements are taken only at discrete time. This distinction is not important for the discussion below, so we will use a continuous time notation, and the results can be easily specialized to discrete time signals.

We often want to characterize what are some statistical properties of the signal $x(t)$. To be able to derive meaningful statistical statements we have to assume that the signal is stationary, meaning that, in some loose sense, its statistical properties are independent of the measurement time. To be more precise, we can interpreter $x(t)$ as a realization of a stochastic process, with well defined statistical properties that are constant over time. under those assumptions we can compute the mean value and the variance of the signal $x(t)$ as expectation values with respect to the underlying properties of the stochastic process

$$m = \mathcal{E}[x] \tag{1.59}$$

$$\sigma^2 = \mathcal{E}[(x-m)^2] \tag{1.60}$$

Clearly, the mean and variance of the signal are not sufficient to characterize completely the signal. In particular, they don't tell us much about the properties of the signal in the frequency domain. For example, the two signals shown here have the same mean of zero, same variance of one, but are very different. In many application it's important to characterize the frequency com-

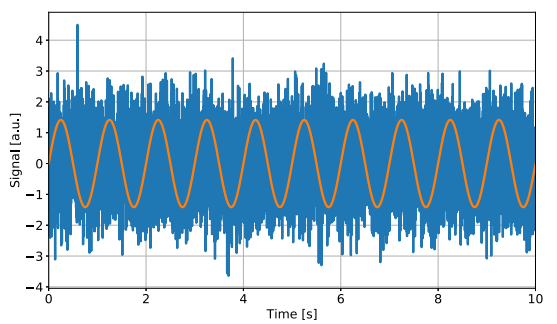

ponent of the signal. If the signal were completely deterministic, we could simply compute the Fourier transform and look at its value at each frequency

$$\tilde{x}(\Omega) = \int x(t) e^{-i\Omega t}\, dt \tag{1.61}$$

Since the signal has some component of randomness in it, we would like to build the frequency dependent equivalent of the signal variance, i.e. some statistica property that tell us how much power there is in the signal at any given frequency. To be more precise, we can define the *power spectral density* (PSD) of the signal, as the distribution of the signal variance with respect to frequency. To be more precise, we can take our signal and band-pass it between two frequencies Ω_1 and Ω_2 to obtain $x_{\Omega_1,\Omega_2}(t)$: this means that we keep only the Fourier components of the signals between the two frequencies, and zero everything else. Then we can compute the variance of the band-pass signal with the same definition used above. If we repeat this operation for all possible pairs of frequencies, we ca build a density function such that

$$\mathcal{E}[x_{\Omega_1,\Omega_2}] = \int_{\Omega_1}^{\Omega_2} S_x(\Omega)\, d\Omega \tag{1.62}$$

The new function $S_x(\Omega)$ is called the (single-sided) power spectral density of the signal x. A more rigorous definition is given by the following expression

$$S_x(\Omega) = \lim_{T\to\infty} \frac{2}{T} \mathcal{E}\left[\left|\int_{-T}^{T} x(t) e^{-i\Omega t}\, dt\right|^2\right] \tag{1.63}$$

The figure on the side shows the PSD of the two signals considered before. Now the different properties of the two signals are evident.

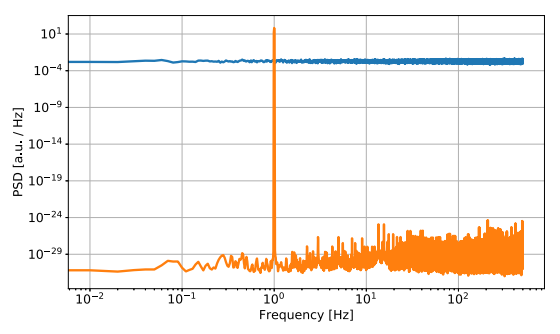

The PSD is a density of the power in the signal. This mean that if the input signal has physical units of, for example, meters m, then the PSD has units of m^2/Hz. Another derived quantity that is often used is the *amplitude spectral density* (ASD) which is simply the square root of the PSD: $S^{1/2}(\Omega)$. The ASD has the strange units of $m/\sqrt{Hz}$ which is a bit baffling at first. But the meaning is simply that the square of the ASD, integrated over a frequency band, gives the total power (or variance) of the signal in that band. Parseval's theorem ensures that

$$\mathcal{E}[x^2] = \int_0^{\infty} S_x(\Omega)\, d\Omega \tag{1.64}$$

where the integral is performed only for positive frequency, hence the name single-sided spectral density.

Shot-noise-limited sensitivity

We are now ready to compute the best achievable sensitivity with a Michelson interferometer. Let's assume a gravitational wave with power spectral density $S_h(\Omega)$ is incident on out Michelson interferometer from the direction perpendicular to the instrument plane, and that it is polarized so that to maximize the coupling to the two arm lengths. We compute above the response of the Michelson interferometer, in the form of a power fluctuation at the anti-symmetric port. The amplitude spectral density of the power fluctuations is simply the product of the interferometer optical gain and the amplitude spectral density of the GW

$$S_P^{1/2}(\Omega) = \left[\frac{4\pi L}{\lambda} r_X r_Y P_i \left|\sin 2k\delta L_0\right|\right] \; S_h^{1/2}(\Omega) \tag{1.65}$$

Here we have neglected the shape of the optical response at very high frequency, as discussed in section 1.1. The absolute value of the sine comes from the fact that the amplitude spectral density is the square root of the power spectral density, and therefore it must be positive. In the previous section we found that this power fluctuation must be contrasted with the quantum limitation given by the shot noise corresponding to the power measured at the anti-symmetric port:

$$S_N^{1/2}(\Omega) = \sqrt{2\hbar\omega P_A} = \sqrt{2\hbar\omega \frac{P_i}{4}\left(r_X^2 + r_Y^2 - 2r_X r_Y \cos 2k\delta L_0\right)} \tag{1.66}$$

The *signal-to-noise ratio* defines our ability to detect the signal: the larger the better, since the power fluctuation due to the GW signal will have a larger amplitude than those due to shot noise:

$$SNR = \frac{S_P^{1/2}}{S_N^{1/2}} = \sqrt{\frac{2\omega}{\hbar c^2}} \cdot \frac{L}{\sqrt{P_i}} \cdot \frac{r_X r_Y \sin 2k\delta L_0}{\sqrt{r_X^2 + r_Y^2 - 2r_X r_Y \cos 2k\delta L_0}} \; S_h^{1/2} \tag{1.67}$$

The minimum gravitational wave amplitude we can detect is for a SNR of one. Therefore we can invert the equation above to give the *shot-noise-limited sensitivity* of the Michelson interferometer: the minimum amplitude of a GW that can be detected with a SNR of one when the instrument is shot-noise limited:

$$S_h^{1/2} > \sqrt{\frac{\hbar c^2}{2\omega}} \cdot \frac{1}{L\sqrt{P_i}} \frac{\sqrt{r_X^2 + r_Y^2 - 2r_X r_Y \cos 2k\delta L_0}}{r_X r_Y \sin 2k\delta L_0} \tag{1.68}$$

This equation contains a lot of information, that needs to be digested to find how to operate the Michelson interferometer to the best of its sensitivity.

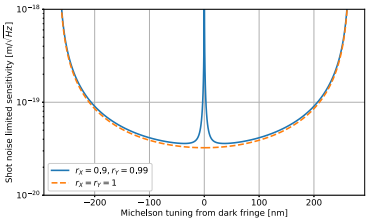

Figure 1.7: Shot-noise-limited sensitivity of a Michelson interferometer with $L = 4$ km, $P_i = 1$ W. The two curves shows two different sets of mirror reflectivities.

- First of all, the shot-noise-limited sensitivity scale with the square root of the laser frequency. So using higher frequencies (shorter wavelength) helps. This is easy to understand, since the wavelength is our reference ruler to measure the distance change due to the GW. So the shorter the wavelength, the larger the GW effect is, compared to our ruler. We don't win linearly with the wavelength, because using higher laser frequencies means that we get less photons for the same power, so the shot noise is worse.
- The sensitivity increase linearly with the length of the arm. This is expected since the effective change in distance due to the GW is proportional to the propagation length. This is of course true until we reach a frequency high enough to be affected by the frequency response described in section 1.1.
- The sensitivity also improves with the square root of the power. The power fluctuation due to a GW is proportional to the total laser power, so we would expect a linear gain in sensitivity. However, as we discussed above, having more photons hitting the detector means that our shot noise is worse. So at the end of the day we gain only proportionally to the square root of the power hitting the beam splitter.
- Finally, depending on the end mirror reflectivity, the optimal tuning of the Michelson fringe changes, see fig. 1.7. We can find the minimum of the shot-noise-limited sensitivity by taking the derivative of eq. 1.68 with respect to δL_0. Assuming that $r_X > r_Y$ we get

$$\delta L_0^{opt.} = \frac{\tan^{-1} \frac{\sqrt{r_X^2 - r_Y^2}}{r_Y}}{2k} \tag{1.69}$$

  As expected, this value gets closer and closer to zero (the dark fringe condition) as the two reflectivity become equal. In practical applications, the two end mirror reflectivities are very close to one, so the best tuning is close to the dark fringe condition. We can approximate $r_X \simeq r_Y \simeq 1$ to compute the best achievable sensitivity, which is obtained for $\delta L_0 \simeq 0$:

$$S_h^{1/2} > \sqrt{\frac{\hbar c^2}{\omega}} \frac{1}{L\sqrt{P_i}} \simeq 1.3 \times 10^{-20} \mathrm{Hz}^{-1/2} \tag{1.70}$$

  where the numerical value has been computed for a 4 km long interferometer and an input power of 1 W.

One question that is left unanswered here is how to practically ensure that the Michelson interferometer is and remains at the right tuning. This is the topic of feedback control system, which is covered in a later chapter.

This number might seem incredibly small, especially considering that it corresponds to a length variation of the order of 5×10^{-17} m/$\sqrt{\mathrm{Hz}}$. However, since the early days of gravitational wave detectors, it was clear that expected astrophysical signals would have been much

weaker than that. Now, after actually detecting gravitational wave signals from the coalescence of compact systems[11] we know to expect amplitude of the order of $S_h^{1/2} \simeq 10^{-22}\mathrm{Hz}^{-1/2}$. Considering that to claim a detection we can't be satisfied with a SNR of one, but we need at least 8 or more, we are missing about three orders of magnitude in sensitivity. How can we get them?

[11] B P Abbott et al. Observation of gravitational waves from a binary black hole merger. *Phys. Rev. Lett.*, 116:061102, 2016; and B P Abbott et al. GW170814: A three-detector observation of gravitational waves from a binary black hole coalescence. *Phys. Rev. Lett.*, 119:141101, 2017

Inspecting eq. 1.70 tells us that we can increase the arm length or increase the laser power. However, it's not feasible from an engineering point of view to have arms much longer than 40 km or so (think of the curvature of the earth), and the currently available best stable lasers have powers of the order of 200 W. Therefore we can only gain a factor $10 \times \sqrt{200} = 140$, even pushing the limit of the current technology. It's clear we need to play some clever tricks to improve the sensitivity, instead of just using brute force.

Shot noise as field noise

In the derivation we gave love for the shot-noise-limited sensitivity, we assumed a specific way to readout the GW signal: that is, we were going to measure the power fluctuations at the anti-symmetric port with a small detuning from the perfect dark fringe.

Here we show that the shot noise limit can be derived in a more general form, which is independent of the readout scheme adopted. First of all, let's go back to the field at the anti-symmetric port, and expand it at first order for small differential length change hL around the working position defined by δL:

$$\begin{aligned} E_A &= -\frac{1}{2}e^{2ikL}\left(r_X e^{ik\delta L} - r_Y e^{-ik\delta L}\right) E_1 \\ &\quad + ikhL\left(-\frac{1}{2}e^{2ikL}\left(r_X e^{ik\delta L} + r_Y e^{-ik\delta L}\right)\right) E_1 \qquad (1.71) \\ &= E_A^{(0)} + gh \qquad (1.72) \end{aligned}$$

where we have defined the new optical gain g for the field. When $r_X \simeq r_Y$ so that our Michelson interferometer has good contrast, the field variation produced by the GW signal is in the same phase with the static field $E_A^{(0)}$, therefore it describes a change in the power carried by the field, proportional to the GW signal

$$E_A = E_A^{(0)}\left(1 + \frac{g}{E_A^{(0)}}h\right) \qquad (1.73)$$

This is the expected behavior from an ideal Michelson interferometer: any change in the differential phase of the two beams recombining

at the beam splitter is converted to a power fluctuation. The absolute phase of the field at any point has no physical meaning, so we can assume that the static field (due for example to the Michelson detuning from dark fringe) is purely real. In the most general case, the field fluctuation due to the GW has a phase difference ϕ with respect to this static reference, so that we can write (defining δE to be real):

$$P = \left| E_0 + e^{i\phi}\delta E \right|^2 = E_0^2 + \delta E^2 + 2E_0\delta E\cos\phi \tag{1.74}$$

Recall that GW signals are extremely weak, so the term δE^2 is negligible and cannot be practically used for detection. But the introduction of the static reference field allowed us to have a power signal which is directly proportional to the GW signal. We can see that the optimal detection gain is obtained when $\phi = 0.$ which is the case if the contrast defect is zero. If r_X and r_Y are different, then the phase is no more zero, and using the power with a Michelson tuning offset to detected the GW signal is no more optimal.

In the most general case we can detect the GW signal ifs we have a way to directly measure the fluctuating part of the field amplitude. The next question therefore is: what is the equivalent of shot noise for the field? With our definition of the units for the field, we have $P = |E|^2$, therefore a fluctuation δP ink power corresponds to

$$P = |E + \delta E|^2 = P\left|1 + \frac{\delta E}{E}\right| \simeq P + 2P\frac{\delta E}{|E|} = P + 2\frac{\delta E}{\sqrt{P}} \tag{1.75}$$

This allows us to write the equivalent of the power shot noise for the field

$$S_E^{1/2} = \frac{S_P^{1/2}}{2\sqrt{P}} = \sqrt{\frac{\hbar\omega}{2}} \tag{1.76}$$

The readers familiar with the quantum description of light will recognize this expression. This field noise is the limiting factor in our ability to detect small GW signals:

$$S_h^{1/2} = \frac{S_E^{1/2}}{|g|} = \sqrt{\frac{\hbar c^2}{\omega}}\frac{2}{L\sqrt{P_i}\sqrt{r_X^2 + r_Y^2 + 2\cos 2k\delta L}} \tag{1.77}$$

This equation is giving us the real fundamental limit on the accuracy we can achieve when measuring a gravitational wave signal in a Michelson interferometer, regardless of the technique we use to actually extract the fluctuating part of the field at the anti-symmetric port. The reader can check that it gives the same value as eq. 1.68 in the optimal case $r_X = r_Y$, and it is always lower in any other case.

Radiation pressure

Photons have no rest mass, but they still carry energy and momentum. For a single photon with energy E, the momentum is $p = \frac{E}{c}$. Therefore, when a photon bounces off a high reflectivity mirror, a momentum $2p$ is transferred to the mirror. One might argue that this number is quite small for a single photon

$$2p = \frac{2E}{c} = \frac{2\hbar\omega}{c} \simeq 10^{-27}\ \mathrm{N\ m} \tag{1.78}$$

but on the other hand there are a lot of photons in beam. If the total power in the beam is P, the *radiation pressure* force exerted on a mirror is

$$F_{RP} = \frac{2P}{c} = 6.7 \times 10^{-9} \left(\frac{P}{1\mathrm{W}}\right)\ \mathrm{N} \tag{1.79}$$

We discussed above that in any laser beam with power P and frequency ω, the quantum fluctuations in the number of photons give rise to a white shot noise with spectrum

$$S_P^{1/2}(\Omega) = \sqrt{2\hbar\omega P} \tag{1.80}$$

Due to radiation pressure, when this beam reflects off a mirror, it will exert a white force noise

$$S_F^{1/2}(\Omega) = \frac{\sqrt{8\hbar\omega P}}{c} \tag{1.81}$$

The effect of this force on a free mirror can be easily computed from the equation of motion of the mirror

$$m\ddot{x} = F \tag{1.82}$$

which in frequency domain becomes

$$\tilde{x}(\Omega) = \frac{\tilde{F}(\Omega)}{-m\Omega^2} \tag{1.83}$$

We can use this equation to convert the force noise spectrum into a displacement spectrum:

$$S_z^{1/2}(\Omega) = \frac{\sqrt{8\hbar\omega P}}{mc\Omega^2} \tag{1.84}$$

Figure 1.8 shows the combination of shot noise and radiation pressure noise for a Michelson interferometer, for a few different input powers. Radiation pressure noise dominates at low frequencies, due to the f^{-2} response of the mirror motion to force. The key thing to note is that while the shot-noise-limited sensitivity improves with

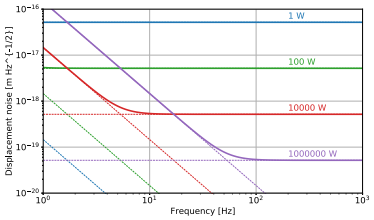

Figure 1.8: Sum of radiation pressure and shot noises for a Michelson interferometer with 1 kg mirrors, for various input power.

$\sqrt{P}$, the radiation-pressure-limited sensitivity gets worse with $\sqrt{P}$. So for each power level, there is a corner frequency at which the two effect are roughly equal, and neither reducing nor increasing the power can improve the sensitivity at that frequency. This is often called the *standard quantum limit* of our displacement measurement.

For a simple Michelson interferometer, radiation pressure starts to be relevant at the frequencies of interest only for very high input power, which are not practically feasible. However, we will see later that, using clever tricks, it is not unreasonable to have $10^5 - 10^6$ W circulating into the interferometer. At that level, radiation pressure starts to be important.

Laser technical noises

In the real world, our instruments are often not limited by fundamental noise sources, but by a pletora of *technical noise*. The distinction between what's fundamental and what's technical is some times a bit murky. Fundamental noise limitations are those that can be overcome only by violating some laws of physics, or changing drastically the instrument design. We will see for example how we can improve on the shot noise by making the interferometer more complex, or using quantum optics techniques. Technical noises are instead due to the limitation in our ability to manufacture components. In this section we consider two such limitations coming from the laser source, namely what happens if the power or the frequency of the laser fluctuate.

Power noise is simple to understand. If the power in input changes with time $P_i(t) = P_0 + \delta P(t)$, the output will change proportionally

$$P_A(t) = P_A \left(1 + \frac{\delta P(t)}{P_0}\right) \tag{1.85}$$

This fluctuation directly translates to a spurious signal that cannot be separated from the GW signals. Ideally, this contribution can be made very small by moving toward the dark fringe condition, since the coupling of laser power noise into the GW signal is directly proportional to the amount of power at the anti-symmetric port. However, in practical application we cannot make the power at the anti-symmetric port as small as we want, since we are ultimately limited by the contrast defect due to imbalances in the two arms. Typical values for a simple Michelson interferometer are at the level of $P_A/P_i \simeq 10^{-4}$. If we write the two end mirror reflectivities as $r_{X,Y} = r \pm \delta r$, then the anti-symmetric port power and the optical

gain are

$$P_A = \frac{P_i}{2}\left[r^2+\delta r^2-\left(r^2-\delta r^2\right)\cos 2k\delta L_0\right] \quad (1.86)$$

$$G = \frac{4\pi}{\lambda}\left(r^2-\delta r^2\right)P_i \sin 2k\delta L_0 \quad (1.87)$$

From the first equation we can see that the minimum power attainable at dark fringe is $P_{min} = P_i\delta r^2$ which means typical values of δr are in the percent range. Assuming $\delta r = 1e-2$, we can use eq. 1.69 to compute the tuning that gives us the best shot-noise-limited sensitivity. We found $\delta L_0 \simeq 17$ nm, that corresponds to $S_h^{1/2} \simeq 3.3\times10^{-20}\mathrm{Hz}^{1/2}$. The power at the anti-symmetric port is $P_A \simeq 9.8\times10^{-4}$ W. We can compute the optical gain, and use the value to convert the shot noise limited sensitivity to equivalent laser power noise

$$S_h^{1/2} = \frac{S_{\delta P_A}^{1/2}}{G} = G^{-1}\frac{\delta P}{P_i}P_A \quad (1.88)$$

and we find that the laser *relative intensity noise* (RIN) that gives a signal of the same amplitude as the shot noise is

$$\frac{\delta P_i}{P_i} < 3\times10^{-12} \quad (1.89)$$

Of course one can always measure the power emitted by the laser using a photodiode, and use a feed-back control system to stabilize it. Ultimately, the achievable performance is limited again by the shot noise in the probe beam. As an exercise, the reader can compute how much power would be needed to reach a shot-noise-limited RIN of 3×10^{-12} as required.

This is incredibly difficult to achieve in lasers. The most stable lasers currently available have a free running RIN of the order of $10^{-6}-10^{-5}$.

Laser frequency noise can also be a problem. Luckily, the Michelson interferometer configuration has a relatively low susceptibility to frequency noise. If the laser frequency changes, the wavelength change accordingly, and therefore the propagation phase accumulated by the laser beam along the arms also changes. The round-trip phase for the X arm is given by $\phi_X = 4\pi L_X/\omega$. If the laser frequency fluctuates by a small amount $\omega = \omega_0+\delta\omega$, the change in phase is $\delta\phi_X/\phi_X = \delta\omega/\omega_0$. Similarly, if the arm length changes by a small amount δL, due for example to a GW passing by, we have as similar change in the round trip phase $\delta\phi_X/\phi_x = \delta L_X/L_X$. Therefore, the effect of a changing laser frequency, for a beam propagating along a distance L, produces an effect on the phase similar to a change of distance, such that:

$$\frac{\delta\omega}{\omega_0} = \frac{\delta L}{L_0} \quad (1.90)$$

The beams propagating along the Michelson arms cannot distinguish the phase fluctuations due to a real distance change, or to the fluctuating laser frequency. The interference at the anti-symmetric port, when close to the dark fringe condition, depends on the difference

of the phase accumulated in the two arms. Therefore, the Michelson interferometer will see a power noise due to frequency noise, proportional to the difference of the two arm lengths

$$\delta L_{(freq.noise)} = (L_X - L_Y)\frac{\delta\omega}{\omega_0} \tag{1.91}$$

This result can also be obtained more formally by making the substitution $\omega \to \omega_0 + \delta\omega$ in eq. 1.42 and expanding at first order in $\delta\omega$. The result is telling us that a Michelson interferometer has a large *common mode rejection* if the two arm macroscopic lengths are made similar. How similar do they need to be? Typical free running noise in stable near infrared lasers is of the order of few 10 Hz/$\sqrt{\text{Hz}}$ at about 100 Hz. This correspond to a fractional stability of $\delta\omega/\omega \simeq 3 \times 10^{-14}$. To ensure that the frequency noise contribution to the Michelson sensitivity is below the shot-noise limit, we have to equalize the two arm lengths at a level of $1.3 \times 10^{-20}/3 \times 10^{-14} = 4 \times 10^{-7}$. For two 4 km long arms, this amounts to about 1.6 mm. Difficult, but not impossible. However, the desired sensitivity to GW signals is about thousand times lower than the simple Michelson shot-noise limit, making it impractical to equalize the distance between the mirror at the micron level.

By now it must be quite clear to the reader that the simple minded approach of increasing the laser power and making the instrument longer does not pay off. If gravitational wave detectors have to reach a sensitivity at the level of $10^{-23}\text{Hz}^{-1/2}$ (and they did), a somewhat more sophisticated approach is needed.

Alternative way to compute the response to frequency noise

If the argument described in the main text is not convincing, we can derive directly the response of a Michelson interferometer to frequency noise, starting from the initial expression for the power at the anti-symmetric port:

$$P_A = \frac{P_i}{4}\left[r_X^2 + r_Y^2 - 2r_X r_Y \cos 2k\Delta L\right] \tag{1.92}$$

where we have retained ΔL in the argument of the cosine, since when we change the laser frequency the resonance condition that defines our initial choice of ΔL_0 changes too. A small change in the laser frequency $\omega \to \omega + \delta\omega$ result in a also small change in the wave vector $k \to w - k\frac{\delta\omega}{\omega}$. We can easily compute the derivative of the power with respect to both a change in length $\Delta L \to \Delta L + \delta L$ and in frequency:

$$\frac{\delta P_a}{\delta\omega} = -\frac{k}{\omega} P_i r_X r_Y \Delta L \sin 2k\Delta L \tag{1.93}$$

$$\frac{\delta P_a}{\delta L} = P_i r_X r_Y 2k \sin 2k\Delta L \tag{1.94}$$

from which it is easy to confirm that the ratio is the same obtained in the text:

$$\frac{\frac{\delta P_a}{\delta\omega}}{\frac{\delta P_a}{\delta L}} = -\frac{\Delta L}{\omega} \tag{1.95}$$

1.4 Fabry-Perot cavities

▷ How can we make the arms longer, with actually making them longer? Or to be more precise, can we find way to increase the optical gain of a simple Michelson interferometer, without resorting to simply making it longer? The answer, as we shall see in this section, is positive. But there is, as always, a price to pay.

Resonance

If the laser beam could bounce multiple time back and forth in the Michelson arms, it would accumulate a larger phase, effectively amplifying the response of the detector to a GW. This could be accomplished using a *delay line* [12] where a laser beam bounces in a zigzag fashion off two mirrors, thus traveling multiple times along the arms. Although this was initially proposed for GW detectors [13], it was turned down in favor of the more powerful and practical resonant Fabry-Perot cavities [14]. Instead of keeping the beams that bounce back and forth separated, we align the mirrors to the same axis, so that all beams overlap. The input mirror (also called input coupler) has a finite transmissivity, so that part or the input beam can couple into the resonant cavity. If the microscopic tuning of the distance between the two mirrors is just right, after each round trip in the cavity, the fields can interfere constructively and build up the standing power into the cavity. Part of the fields will be transmitted back through the input mirror, and out of the cavity, providing a probe that carries information on the phase accumulated into the multiple round-trips. Figure 1.9 shows a simple scheme of a resonant Fabry-Perot cavity, with all the fields involved. With computations similar to what we have done for the Michelson interferometer, we can write down the relations between all fields, with particular attention to the transmitted field E_t and the reflected field E_r.

$$E_1 = t_i E_i + r_i E_4 \tag{1.96}$$
$$E_4 = e^{2ikL} r_e E_1 \tag{1.97}$$
$$E_r = t_i E_4 - r_i E_i \tag{1.98}$$
$$E_t = e^{ikL} t_e E_1 \tag{1.99}$$

where again the minus sign in the second equation is due to the fact that the input beam is reflecting off the secondary side of the mirror. Those equations are a set of relations that must be true for the field once the cavity has reached a stationary state. We often neglect the fast transient that happens in a cavity, for example when the laser is suddenly switched on, and focus on the *quasi-static* approximation,

[12] Donald R. Herriott and Harry J. Schulte. Folded optical delay lines. *Appl. Opt.*, 4(8):883–889, Aug 1965. DOI: 10.1364/AO.4.000883. URL `http://ao.osa.org/abstract.cfm?URI=ao-4-8-883`

[13] D. Shoemaker, R. Schilling, L. Schnupp, W. Winkler, K. Maischberger, and A. Rüdiger. Noise behavior of the garching 30-meter prototype gravitational-wave detector. *Phys. Rev. D*, 38:423–432, Jul 1988. DOI: 10.1103/PhysRevD.38.423. URL `https://link.aps.org/doi/10.1103/PhysRevD.38.423`

[14] A. Perot and C. Fabry. On the Application of Interference Phenomena to the Solution of Various Problems of Spectroscopy and Metrology. *Astrophysical Journa*, 9:87, February 1899. DOI: 10.1086/140557

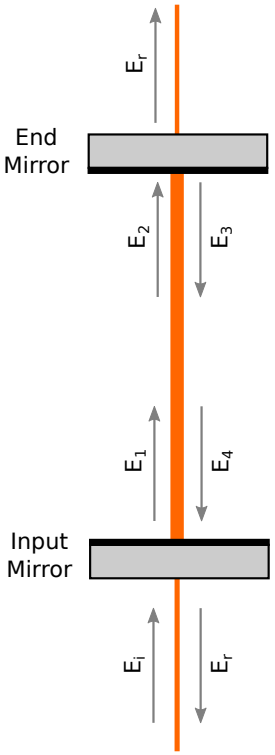

Figure 1.9: A Fabry-Perot cavity, with the main fields involved in the computation.

which assumes that all changes in the optical parameters (length of the cavity, mirror reflectivities, laser power, etc.) are happening slow enough so that any transient can be neglected. We can find the quasi-static field as the self consistent solution of the above set of equations:

$$E_1 = \frac{t_i}{1 - r_i r_e e^{2ikL}} E_i \tag{1.100}$$

$$E_t = \frac{t_i t_e e^{ikL}}{1 - r_i r_e e^{2ikL}} E_i \tag{1.101}$$

$$E_r = -\frac{r_i - r_e(r_i^2 + t_i^2) e^{2ikL}}{1 - r_i r_e e^{2ikL}} E_i \tag{1.102}$$

Let's focus first on the intra-cavity field. The power inside the cavity depends on the microscopic tuning of the cavity length from resonance, that we shall call δL. As in the Michelson interferometer case, the macroscopic value of the length L_0 does not matter as long as we choose it to be a multiple of $\lambda/2$. Starting from eq. 1.100 we can compute the intra-cavity power as $P_1 = |E_1|^2$:

$$P_1 = \frac{t_i^2}{(1 - r_i r_e)^2} \frac{1}{1 + \frac{4 r_i r_e}{(1 - r_i r_e)^2} \sin^2 k\delta L} P_i \tag{1.103}$$

As shown in fig. 1.10, the power inside the cavity exhibits a narrow resonance peak, centered around the zero microscopic tuning of the cavity length. The width of the resonance peak depends only on the mirror parameters. The half width at half maximum of the peak can be easily computed from eq. **??**:

$$\delta L_{HWHM} = \frac{\lambda}{2\pi} \arcsin\left(\frac{2\sqrt{r_i r_e}}{1 - r_i r_e}\right)^{-1} \tag{1.104}$$

In most practical cases, the resonance width is much smaller than the *free spectral range*, that is the distance between two consecutive distances $\delta L_{FSR} = \lambda/2$. Therefore the argument of the arcsine is small, and we can use the following approximation:

$$\delta L_{HWHM} \simeq \frac{\lambda}{2} \frac{1}{2\frac{\pi\sqrt{r_i r_e}}{1 - r_i r_e}} = \frac{\lambda}{2} \frac{1}{2\mathcal{F}} \tag{1.105}$$

where the last identity defines the *cavity finesse* $\mathcal{F} = \frac{\pi\sqrt{r_i r_e}}{1 - r_i r_e}$, which gives the ratio between the free spectral range and the full linewidth of the resonance peak. Typical numbers for the resonant cavities used in gravitational wave detectors range from $\mathcal{F} \sim 50 - 150$ for first generation detectors, to $\mathcal{F} \sim 450 - 1500$ for the second generation detectors. One can invert the relation between the mirror reflection coefficient and the finesse:

$$r_i r_e = 1 - \frac{\pi}{\mathcal{F}} + \mathcal{O}\left(\frac{1}{\mathcal{F}^2}\right) \tag{1.106}$$

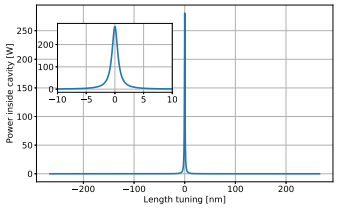

Figure 1.10: Power into a Fabry-Perot resonant cavity, with 1 W in input, high reflectivity end mirror and $T_i = 0.014$. The inset shows a zoomed-in version in the x axis.

so that an alternative way to compute the finesse, when it's large, is the following expression:

$$\mathcal{F} \simeq \frac{\pi}{1 - r_i r_e} \tag{1.107}$$

The maximum power build-up, at the peak of the resonance, is given by

$$P_1^{(max)} = \frac{t_i^2}{(1 - r_i r_e)^2} P_i \simeq \frac{2\mathcal{F}}{\pi} P_i \tag{1.108}$$

where the approximated equality is valid when the finesse is high, and the mirror reflectivity is very close to unity $r_e \simeq 1$. One way to interpreter this increase of circulating power is to imagine the beams to propagate over multiple effective round-trips. The build-up factor $2\mathcal{F}\pi$ can then be interpreted as the number of round-trips inside the cavity.

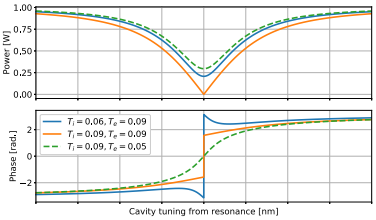

Figure 1.11: Power reflected by a Fabry-Perot cavity with three different set of mirror reflectivities.

So far we just proved that Fabry-Perot cavities are an efficient way to store more circulating power, but it is not clear at all why they should help us with the detection of gravitational waves. To understand this, let's turn our attention to the reflected field, shown in eq. 1.102 and in fig. **??**. The power in reflection always hits a minimum at resonance. However, it's clear that there are three distinct cases to be considered. The reflected field is the interference of two components: this prompt reflection from the back of the input mirror (which has constant phase) and the leakage field from inside the cavity through the input mirror (which has a phase that rotates a full 2π when the cavity tuning changes over a free spectral range). Depending on the balance between the input and end mirror reflectivities we have:

For simplicity here we ignore the optical losses in the input mirror and assume that $r_i^2 + t_i^2 = 1$, but the discussion holds even in that case.

- When $r_i > r_e$ ($t_i < t_e$) the prompt reflected beam always dominates over the leakage beam, so the phase of the reflected beam rotates, but always keep close to the negative sign. This is called an *under-coupled cavity*.
- When $r_i < r_e$ ($t_i > t_e$) the leakage field dominates, so the phase of the reflected beam rotates a full 2π, changing sign between resonance and off-resonance. This is called an *over-coupled cavity*.
- When $r_i = r_e$ ($t_i = t_e$) the reflected field goes exactly to zero when the cavity cross resonance. Cleary, all that power must go somewhere, so it is mostly transmitted through the end mirror. This is called an *optimally coupled cavity* (or impedance matched, using terminology borrowed from the electronic engineering world).

In both the over-coupled or under-coupled cases, most of the power is reflected back. Out of resonance, the leakage field from the cavity

is small, so the prompt reflection dominates: the reflected field has a minus sign, as expected from the reflection on the back side of the input mirror. At resonance, the reflected power is reduced to a small value, which is determined by the total optical loss inside the cavity: the absorption and scattering loss of the two mirror and the transmission for the end mirror. Indeed, if the input and end mirror losses L_i and L_e are small, we can expand the reflected power at first order in L_i and L_e and find, for a high finesse cavity

Here we account for the end mirror transmission in the total loss L_e.

$$P_R = P_i \left[1 - \frac{2\mathcal{F}}{\pi} (L_i + L_e) \right] \tag{1.109}$$

and we can therefore interpreter $L_i + L_e$ as the total round trip loss and $\frac{2\mathcal{F}}{\pi}$ as the number of round trips the field propagate inside the cavity.

We can finally understand how a Fabry-Perot cavity can help us in detecting GWs. From fig. 1.11 it is apparent that in a over-coupled cavity, the phase of the reflected field rotates quite rapidly when the cavity length is changed close to resonance. We can expand eq. 1.102 at first order in the cavity displacement δL, assuming for simplicity that $L_i = 0$:

$$E_R(\delta L) = \frac{r_i - r_e}{1 - r_i r_e} + 2ik\delta L \frac{r_e(1 - r_i^2)}{(1 - r_i r_e)(r_e - r_i)} + \mathcal{O}\left(\delta L^2\right) \tag{1.110}$$

If we factor out the value of the reflected field at resonance $E_r^{(res)}$, we can recognize that at first order the effect of a small cavity length change is purely imaginary, confirming that only the phase is changed. In the approximation $r_e \simeq 1$ we find

$$E_r = E_r^{(res)} \left(1 + 2ik \frac{2}{1 - r_i} \delta L \right) = E_r^{(res)} e^{i\phi_{FP}(\delta L} \tag{1.111}$$

where we defined the phase of the field reflected from a Fabry-Perot cavity as

$$\phi_{FP}(\delta L) = 2k \frac{2}{1 - r_i} \delta L = 2k \frac{2\mathcal{F}}{\pi} \delta L \tag{1.112}$$

If we removed the input mirror, and let the beam propagate to the end mirror and back to the origin, the accumulated phase would have simply been $\phi_{free} = 2k\delta L$, since all that matters is the microscopic change in the distance. Therefore, by having a Fabry-Perot cavity, we can amplify the effect of a small length change on the laser field by a factor $\frac{2\mathcal{F}}{\pi}$. This further strengthen out intuition that this is indeed the number of round trips the laser beam do in the cavity: at each round trip the field accumulates a phase $2k\delta L$.

So here is our first magic trick. If we take out Michelson interferometer, and substitute the 4 km long arms with 4 km long over-coupled Fabry-Perot cavities, we can optically amplify the phase

of the two fields impinging back on the beam splitter by $\frac{2\mathcal{F}}{\pi}$. In the second generation detectors Advanced LIGO and Advanced Virgo, the arm cavities have finesse of 450, which gives us an optical gain of about 286 over a simple Michelson interferometer. If every else remained the same, this would amplify the signal due to a GW by this same amount. Unfortunately, there are always prices to pay for any such improvement. The first one, which will be discussed in a later chapter, is that to profit from this gain, we have to maintain the microscopic tuning of the cavity as close as possible to the resonance condition. The second, more fundamental price to pay, is discussed in the next section.

Frequency response

We already discussed in section 1.1 that there is a frequency dependent component in the response to GW of the distance between free falling masses. However, we saw that for practical distance of a few km, this is negligible for audio frequencies, i.e. below some tens of kHz. Unfortunately, Fabry-Perot cavities introduce another frequency dependency, which turns out to be important for km-scale detectors.

Let's assume that the (microscopic) distance between the input and end mirrors is changing in a sinusoidal fashion with a frequency Ω, or with a period $2\pi/\Omega$. The laser beam propagates inside the cavity for about $2\mathcal{F}/\pi$ round trips, each of them taking a time $2L/c$. Therefore, the distance fluctuations are effectively averaged over a time $T = \frac{4\mathcal{F}L}{\pi c}$. Therefore we expect to see a degradation of the response when the averaging time is comparable with the GW period:

$$\frac{c}{2L} \times \frac{2\mathcal{F}}{\pi} \sim \frac{2\pi}{\Omega} \tag{1.113}$$

or for frequencies of the order of $f_{GW} \sim \frac{\pi}{2}\frac{c}{2\mathcal{F}L}$. For a 4-km long Fabry-Perot cavity with a finesse of 450, this frequency is about 100 Hz. So it looks like a Fabry-Perot cavity can increase the response of a Michelson interferometer to GWs, but only at low frequencies.

Let's be more precise and compute the full frequency response of a Fabry-Perot cavity. To do this, we consider a very small cavity motion at a single frequency:

$$L \to L + z(t) = L + z_0 \cos \Omega t \tag{1.114}$$

This distance variation can be oriented in many different ways: a gravitational wave actually changing the local metric, or a physical motion of one of the cavity mirrors.

and study the effect on the propagation over the cavity length L. This length variation causes the phase of the propagated beam to gain an additional time varying component. Since $\left|\frac{z_0}{\lambda}\right| \ll 1$ we can expand at

first order in z_0

$$\begin{aligned} E_L &= E_0 e^{iKL - i\omega t + ikz_0 \cos\Omega t} \\ &= E_0 \left[e^{-i\omega t} + \frac{ikz_0}{2} \left(e^{-i(\omega+\Omega)t} + e^{-i(\omega-\Omega)t} \right) \right] \end{aligned} \quad (1.115)$$

The field behaves like the sum of three components: one oscillating at the main laser frequency ω, called the *carrier field*, and two oscillating at the neighboring frequencies of $\omega \pm \Omega$, called *signal sidebands* or *audio sidebands*. The sidebands have an amplitude which is proportional to the amplitude of the distance variation z_0 and to the carrier field inside the cavity $\delta E(\Omega) = ikz_0/2$, and frequencies that are shifted by a small amount with respect to the carrier. At any position, the laser field is indeed made of three components at a different frequency. Since the laser field must still be a solution of the wave equation, the audio sidebands behave for all purposes like additional fields with frequencies $\omega \pm \Omega$: when they propagate over a distance L, they acquire a phase $\frac{\omega \pm \Omega}{c} L$. This phase should not be confused to the time varying phase produced by the distance variation: first, the time-varying change in distance generates two signal sidebands, then those two sidebands propagate inside the interferometer, behaving like fields at frequencies $\omega \pm \Omega$.

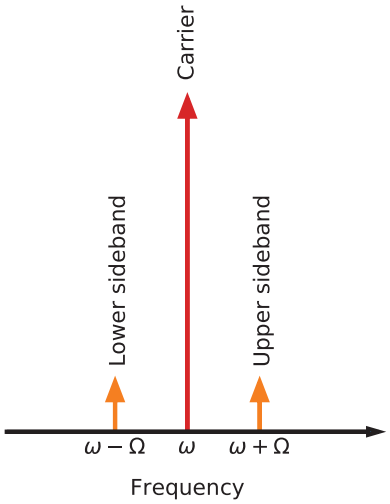

Figure 1.12: Schematic representation of the carrier and signal sidebands generated by a time-varying distance.

The term audio sidebands has nothing to do with the acoustic origin of the signal. It is often used to contrast audio sidebands (generated by mirror motion or GWs at audio frequencies up to a few kHz) with radio-frequency sidebands (with frequencies in the MHz region).

Armed with this signal sidebar description, we can compute the response of a Fabry-Perot cavity to a monochromatic length change. Figure 1.13 shows a schematic of the fields involved. For simplicity we assume that the change in length is due to a motion $z(t) = z_0 \cos\Omega t$ of the end mirror, but a similar derivation can be carried out for an input mirror motion or for a "distributed" change in distance due to a GW. The field reflected from the end mirror is

$$\begin{aligned} E_3 &= r_e E_2 e^{2ikz_0 \cos\Omega t} \simeq r_e E_2 \left[1 + ikz_0 \left(e^{i\Omega t} + e^{-i\Omega t} \right) \right] \\ &= E_3 + \delta E_3(\Omega) + \delta E_3(-\Omega) \end{aligned} \quad (1.116)$$

The additional signal sidebands then propagate inside the cavity and interfere back on the end mirror to create the self-consistent signal fields. Here we focus only on the sideband at $+\Omega$, but similar results hold for the sideband at $-\Omega$:

$$E_3(\Omega) = \frac{\delta E_3(\Omega)}{1 - r_i r_e e^{2ikL - 2i\frac{\Omega}{c}L}} \quad (1.117)$$

and from this we can compute the signal sideband field in reflection from the cavity:

$$E_r(\Omega) = t_i e^{ikL + i\frac{\Omega}{c}L} E_3(\Omega) \quad (1.118)$$

$$= \left[\frac{t_i e^{ikL}}{1 - r_i r_e e^{2ikL}} E_i \right] \frac{r_e t_i e^{ikL - i\frac{\Omega}{c}L}}{1 - r_i r_e e^{2ikL - 2i\frac{\Omega}{c}L}} ikz_0 \quad (1.119)$$

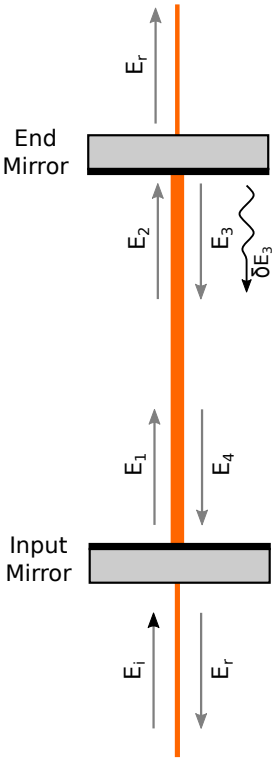

Figure 1.13: A Fabry-Perot cavity, with an audio sideband source inside the cavity.

The term in the square brackets just describe the power build-up inside the Fabry-Perot cavity, which as already described above is maximum at resonance and independent of the signal frequency. But the second term is dependent on the signal frequency. At resonance, we have $e^{2ikL} = 1$, so the response of the signal sidebands in reflection simplifies to

$$E_r(\Omega) = \frac{t_i E_i}{1 - r_i r_e} \frac{r_e t_i e^{-i\frac{\Omega}{c}L}}{1 - r_i r_e e^{-2i\frac{\Omega}{c}L}} ikz_0 \tag{1.120}$$

The phase at the numerator $e^{1\frac{\Omega}{c}L}$ is accounting for the fact that the motion is happening at the end mirror, and it is therefore delayed when it reaches the reflection port. This phase is small for frequencies in the audio bands, even for km-scale cavities. The effect of the same phase at the denominator is however very different. If the signal frequency is small, we can expand the exponential and write

$$E_r(\Omega) = \frac{r_e t_i^2 E_i}{(1 - r_i r_e)^2} \frac{1}{1 - i\frac{r_i r_e}{1 - i r_i r_e}\frac{\Omega}{\frac{c}{2L}}} ikz_0 \tag{1.121}$$

In the case of large finesse, using eq. 1.107, this can be further simplified to

$$E_r(\Omega) = ikz_0 r_e E_i \frac{2\mathcal{F}}{\pi} \frac{1}{1 - i\frac{\Omega}{2\pi\frac{c}{4\mathcal{F}L}}} \tag{1.122}$$

The frequency dependency is described by a first order low pass filter, with a corner frequency given by (the *cavity pole frequency*)

$$f_{cav} = \frac{c}{4\mathcal{F}L} \tag{1.123}$$

For a Fabry-Perot cavity like those used in Advanced LIGO, we have $L = 4$ km, $\mathcal{F} \simeq 450$, so $f_{cav} \simeq 42$ Hz. Compare this result with out first estimate of the cavity bandwidth, eq. 1.113. Our guesswork gave a result pretty close to the real value. Note that at the cavity pole frequency the cavity response decreases of a factor $\sqrt{2}$ with respect to the maximum, which happens at low frequency.

An alternative way to understand the low pass effect of a Fabry-Perot cavity, is to think in terms of the signal sidebands. Since they have a different frequency, they also accumulate a phase shift in each round-trip that differs from the main carrier field. This shift is equivalent to moving the cavity slightly our of resonance for the signal sideband. When the frequency is comparable to the line-width of the cavity, we start seeing a degradation of the signal sideband build-up into the cavity, and therefore a reduced response in reflection.

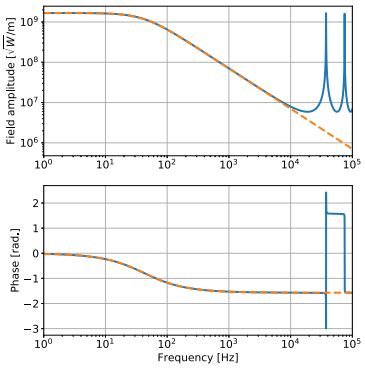

Figure 1.14: Frequency response of a Fabry-Perot cavity: field amplitude in reflection for unit input power and unit displacement of the end mirror. The solid curve shows the exact functional shape, while the dashed curve is the low frequency approximation described in the text.

Gravitational waves in the signal sideband formalism
We can describe the effect of a GW on the field propagating through space using the signal sideband formalism. We expect that the effect of the "distributed" distance change due to the GW is the creation of signal sidebands proportional to the GW amplitude. Let's start by considering the carrier field propagating over a distance L. If we call $E(0)$ the field at the origin, without any GW the field at a distance z is given by

$$E(z) = E(0)e^{ikz} \tag{1.124}$$

Since the effect of the GW is distributed along the entire propagation, we have to take into account the generation of signal sideband at all positions. In presence of a gravitational wave $h(t) = h_0 \cos \Omega t$, the propagation from z to $z + dz$ takes the form

$$E(z+dz) = E(z)e^{ikdz(1+\frac{h(t)}{2})} = E(z)e^{ikdz}\left(1 + ik\frac{h_0}{2}dz\frac{e^{-i\Omega t} + e^{i\Omega t}}{2}\right) \tag{1.125}$$

Therefore, at each position z the gravitational wave generate signal sidebands with amplitude (at first order in dz):

$$dE_z(z) = \frac{ikh_0 dz}{4}E(z) = \tag{1.126}$$

that then propagates to the final position $z = L$

$$dE_z(L) = \frac{ikh_0 dz}{4}E(z)e^{ik(L-z)+i\frac{\Omega}{c}(L-z)} \tag{1.127}$$

The total signal sideband at the position L is therefore given by the sum of all contributions:

$$\begin{aligned} \delta E(L) &= \int_0^L dE_z(L) = \frac{ikh_0}{4}E(0)e^{ikL}\int_0^L e^{i\frac{\Omega}{c}(L-z)}dz \\ &= \frac{ikh_0 L}{4}E(0)e^{ikL}e^{i\frac{\Omega L}{2c}}\operatorname{sinc}\frac{\Omega L}{2c} \end{aligned} \tag{1.128}$$

The final result is the same we found in section 1.1, now expressed in terms of signal sidebands.

1.5 *Michelson interferometer with Fabry-Perot cavities*

▷ It is time to put together the two ideas we explored so far, i.e. to build an GW detector with a Michelson interferometer where the two arms are resonant Fabry-Perot cavities. We shall see how this improves the sensitivity of the detector.

Summarizing, a over-coupled Fabry-Perot cavity has a reflectivity which is close to unity for the carrier field, so it behaves in a ways which is very similar to a high reflectivity mirror. The power stored inside the cavity is amplified with respect to the input power, by a factor which is proportional to the cavity finesse. The same amplification applies to the phase response of the reflected beam to GWs, but only for frequencies below the cavity pole. Therefore, if we substitute the arms of a Michelson interferometer with Fabry-Perot resonant

cavities, we gain sensitivity, at least at low frequencies.

To describe a Fabry-Perot-Michelson interferometer, we could write all the fields equations as we did in the previous configuration, and solve them. However, we can treat each Fabry-Perot cavity as a sort of black box: an optical system with known input-output relations. In particular, to build the field and response of the Fabry-Perot-Michelson, we need two components:

- The Fabry-Perot cavity reflectivity for the carrier field, given in eq. 1.102, which will play the role of the two end mirror reflectivities in the Michelson interferometer equation.
- The response of the field phase in reflection to a gravitational wave signal, as given by eq. 1.122. We expressed the response in terms of audio sidebands, but to compare it with a simple Michelson interferometer, it is easier to express it in terms of the phase of the reflected field as a function of the GW amplitude. Equation 1.122 shows that the signal sidebands are purely imaginary, meaning that they described a phase modulation of the field:

$$\phi_{FP} = kLhr_e \frac{2\mathcal{F}}{\pi} \frac{1}{1 - i\frac{\Omega}{2\pi \frac{c}{4\mathcal{F}L}}} \tag{1.129}$$

  where L is now the length of the arm cavity. This is to be compared with the phase modulation on one arm of a simple Michelson

$$\phi_{space} = kLh \tag{1.130}$$

We can therefore go back to the expression for the optical gain of a Michelson interferometer in eq. 1.131 and simply substitute the Fabry-Perot response into it:

$$G(\delta L_0) = \frac{8\pi\mathcal{F}L}{\lambda} \frac{1}{1 - i\frac{\Omega}{2\pi \frac{c}{4\mathcal{F}L}}} r_X r_Y P_i \sin 2k\delta l \tag{1.131}$$

where now r_X and r_Y are the Fabry-Perot cavity reflectivities for the carrier field, which are practically one for low optical loss cavities, and δl is the microscopic tuning of the differential length of the two Michelson arms, i.e. the difference of the distances between the beam splitter and the two input mirrors. Now we have three different tunings to take care of:

- The Michelson interferometer tuning δl: which is the microscopic component of the difference of the distance between the beam splitter and the two input mirrors. The same arguments we used to find the optimal tuning in the simple Michelson case can be used here.

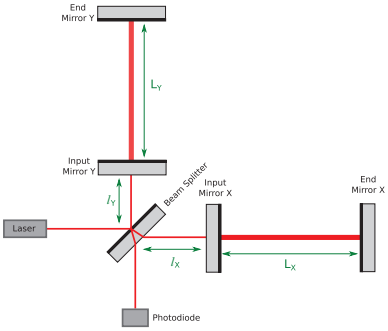

Figure 1.15: A Michelson interferometer with Fabry-Perot arms.

If we have a phase modulation of a field, like for example $E_0 e^{im\cos\Omega y}$, then for a small modulation depth m, we can always expand the exponential and get a signal sideband expression for the phase modulation which is $E_0\left(1 + ime^{-i\Omega t} + ime^{i\Omega t}\right)$.

- The two arm cavity tunings. We already discussed above that the maximum sensitivity to a GW signal is obtained when both cavities are at resonance.

As a side note, instead of detuning the Michelson interferometer from dark fringe by changing δl, we could add a small differential detuning to the two arm cavities. Due to phase amplification property of the Fabry-Perot cavity, this is equivalent to a larger Michelson detuning, without significantly affecting the frequency response of the arm cavities.

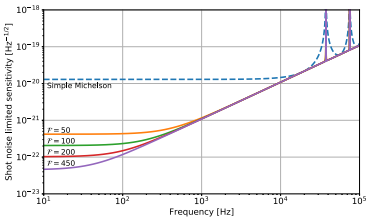

Figure 1.16: Shot-noise-limited sensitivity achievable with a Fabry-Perot-Michelson interferometer. The traces shown here include the high frequency response of the propagation phase to GW, computed in section 1.1.

We can compute the shot-noise-limited sensitivity of a Fabry-Perot Michelson interferometer and compare it with a simple Michelson interferometer. Figure 1.16 shows the result for a few values of the cavity finesse, and compares it with the sensitivity achievable with a Michelson interferometer without cavities. Here we factored in the high-frequency response of the phase to a GW, that we computed in 1.1. In conclusion, using resonant cavities in the arms we can increase the detector sensitivity at all frequencies, but we can get a significant improvement only at low frequencies. This is one of the reasons why first generation detectors used relatively low value for the finesse (50-200), to avoid narrowing too much the detector bandwidth. Of course, if shot noise were the only factor to limit the sensitivity, it would make sense to have a high a finesse as possible. But in a real world system, as we shall see in a later chapter, there are sources of noise that contribute mostly at low frequency, therefore it does not pay off to increase the finesse too much. Second generation detectors such as Advanced LIGO use higher finesse (450 and higher) which would result in a very narrow bandwidth of the detector. But this problem is solved using another optical trick, namely a signal recycling cavity. But that will have to wait a bit more.

1.6 *Power recycling*

▷ *In a Michelson interferometer tuned at dark fringe, no power is exiting through the anti-symmetric port, and if the end mirrors (or the arm cavity) have low enough power losses, all the power is reflected back to the symmetric port, which is at a bright fringe condition. All that wasted power...*

Power recycling gain

When the Michelson interferometer is tuned at a dark fringe condition for the anti-symmetric port, the symmetric port is tuned at a bright fringe. Therefore, conservation of energy implies that all

the input power goes either one of two ways: if it's not absorbed or scattered somewhere inside the interferometer, it is going back toward the laser. The basic idea of *power recyling* is to add another semi-transparent mirror at the symmetric port, between the laser and the beam splitter. This mirror will reflect back part of the beam, that can then recombine with the main beam and increase the circulating power. To be more precise, we can tune the distance between the beam splitter and this *power recycling mirror* (PRM) in such a way to ensure that the all beams reflected back interferes constructively, thus effectively creating a new Fabry-Perot resonant cavity, composed of the power recyling mirror and a "virtual" mirror made of the Michelson interferometer.

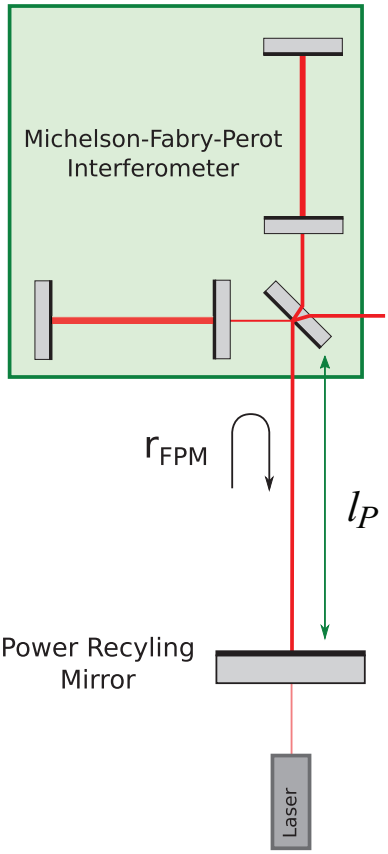

Figure 1.17: Schematic diagram of a power-recycled Fabry-Perot-Michelson interferometer.

Let's build an accurate description of a power-recycling Fabry-Perot-Michelson interferometer step by step. First of all, recall that the reflection of a over-coupled Fabry-Perot cavity with high finesse and low optical loss, at resonance, is given by eq. 1.102, which at first order in the optical loss can be simplified to

$$r_{FP} = -1 + \frac{\mathcal{F}}{\pi}\left(L_i + L_e\right) \tag{1.132}$$

We can use this as the reflectivity of the end mirrors in a Michelson interferometer to compute the field at the symmetric port, using eq. 1.41, and enforcing the dark fringe condition for the anti-symmetric port, which we know is very close to the desired working condition:

$$E_S = \frac{E_i e^{2ikl}}{2}\left(r_{FP}^{(X)} + r_{FP}^{(Y)}\right) \tag{1.133}$$

where l is the average length of the two Michelson short arms $l = \frac{l_X + l_Y}{2}$. If we assume the two Fabry-Perot cavity to be equal, we can further simplify the expression above. We see that the Fabry-Perot-Michelson, as seen from the symmetric port, behaves like an effective mirror with complex reflectivity given by

$$r_{FPM} = -e^{2ikl}\left(1 - \frac{\mathcal{F}}{\pi}L_{RT}\right) \tag{1.134}$$

where $L_{RT} = L_i + L_e$ are the total round-trip losses into the arm cavity. If we insert a power recycling mirror between the laser and the rest of the interferometer, we are forming a resonant cavity (called the *power recycling cavity* or PRC). The field circulating inside this cavity is given by the usual expression:

$$E_{PRC} = \frac{t_p}{1 - r_p r_{FPM} e^{2ikl_P + 2ikl}} E_{in} \tag{1.135}$$

where l_P is the tuning of the distance between the power recycling mirror and the beam splitter. The resonance condition into the power

recycling cavity is determined by the round-trip phase due to propagation over a distance

$$l_{PRC} = l_P + \frac{l_X + l_Y}{2} \tag{1.136}$$

which is usually called the *power recycling cavity length*. At resonance, the circulating power is given by

$$P_{PRC} = \frac{1 - r_p^2}{\left[1 - r_p\left(1 - \frac{\mathcal{F}}{\pi} L_{RT}\right)\right]^2} P_{in} \tag{1.137}$$

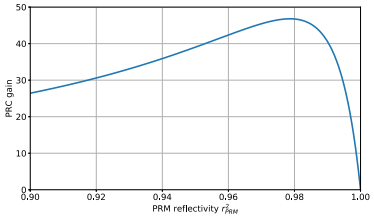

Figure 1.18: Power recycling gain for a power-recycled Fabry-Perot-Michelson with arm cavity finesse of 450, and arm cavity round trip losses of 75 ppm.

Figure 1.18 shows the *power recycling gain* (i.e. the ratio of the power circulating inside the power recycling cavity to the input laser power) as a function of the power recycling mirror reflectivity, for a configuration where the arm cavities have finesse of 450 and round trip losses of 75 ppm. It is apparent that the gain is maximum for a particular value of the power recycling mirror reflectivity, which can be found but equating the derivative of the gain to zero

$$r_p^{(optimal)} = 1 - \frac{\mathcal{F}}{\pi} L_{RT} \tag{1.138}$$

which corresponds to matching the power recycling mirror reflectivity to the equivalent reflectivity of the Fabry-Perot-Michelson interferometer. The maximum value of the recycling gain, at first order in the arm cavity loss is

$$G_{PRC}^{(optimal)} = \frac{\pi}{2\mathcal{F} L_{RT}} \tag{1.139}$$

The peak is quite broad, so a fine tuning is not necessary. This is good news, since it is often quite difficult to estimate the total round trip loss in a cavity, before actually building it. This choice of the power recycling mirror reflectivity makes the power recycling cavity an optimally coupled Fabry-Perot cavity, meaning that the reflected field is zero. So in this configuration there is no power reflected back to the laser. But where is all the input power going? One can easily show with detailed computation, or from simple energy balance, that the entire input power is lost in the arm cavities due to L_{RT}. Indeed, for 1 W in input, the power circulating into the power recycling cavity is given by G_{PRC}, meaning that each Fabry-Perot cavity has a power of $G_{PRC}/2$ in input. This power is bouncing back an forth into the arms $2\mathcal{F}/\pi$ times, each time incurring a power loss of L_{RT}. Therefore the total power lost in the arms is

$$P_{in} \times \frac{\pi}{2\mathcal{F} L_{RT}} \times \frac{1}{2} \times 2 \times \frac{2\mathcal{F}}{\pi} L_{RT} = P_{in} \tag{1.140}$$

This result also suggests that to obtain the highest possible recycling gain, one has to keep the arm cavity round trip loss as low as possible. State of the art mirrors for the second generation of GW interferometric detectors achieved $L_{RT} \sim 75 - 100$ ppm (parts per million). Given the expected round trip loss, choosing a too high finesse will result in a reduced power recycling gain.

Response to GW signals

The discussion so far showed that the power recycling technique is broadly equivalent to an increased input laser power. However, we have not discussed what is the effect of the addition of the power recycling cavity to the response to gravitational wave signals. We will show here that there is no effect, apart from the effective increase of power.

Let's consider a gravitational wave propagating across our detector. As usual, for simplicity, we assume that the GW propagates along the direction perpendicular to the detector plane, and is optimally polarized, so to create a maximal differential length change in the two arms. The net effect of the GW is to create signal sidebands inside each arm cavity, with an amplitude proportional to the power circulating inside the arm, and to a frequency dependent component described by the cavity pole. Since the GW effect is differential, the signal sidebands created in the X arm will have opposite sign with respect to those created in the Y arm. Those two pair of signal sidebands will then propagate out of the Fabry-Perot cavities and recombine at the beam splitter. Here, the fact that the two set of sidebands have opposite sign implies that their interference condition at the beam splitter is reversed with respect to the carrier field. For the signal sidebands the Michelson is tuned so to have bright fringe at the anti-symmetric port, and dark fringe at the symmetric port. This means that the signal sidebands will maximally propagate to the anti-symmetric port, and minimally to the symmetric port and the power recycling cavity. It is then clear that the power recycling cavity has no effect on the interferometer response to GWs, except for the effective increase of the power impinging on the beam splitter.

Therefore we can compute the shot-noise limited sensitivity of a power recycled Fabry-Perot Michelson quite simply, by just rescaling the power by the recycling gain. In other words, we gain an increase in sensitivity proportional to the square root of the recycling gain, which is almost a factor 7 for the numbers we computed above.

The power recycled Fabry-Perot-Michelson interferometer was

the configuration used in the first generation of gravitational wave detectors, like initial LIGO, Virgo and TAMA. For those detectors the arm cavity finesse was 150-200, and the best recycling gain that could be obtained was about 30. With an input power of about 10 W, this resulted in a shot-noise-limited sensitivity of about 5×10^{-23} $\mathrm{Hz}^{-1/2}$ at low frequency, with a corner at the cavity pole at about 100 Hz.

Common mode signals filtering

Using a power recycling cavity has another advantage over simply using a higher power laser. Indeed, although power recycling has no effect on the differential signals generated by GWs, it does have an important filtering effect on *common mode* signals, such as laser frequency and power noise.

First of all, let's see how we can express laser noises in terms of signal sidebands. The instantaneous laser frequency can bee defined as the derivate of the field phase, at a fixe position, with respect to time

$$\omega = \frac{d\phi}{dt} \tag{1.141}$$

If we consider a monochromatic perturbation to the laser frequency $\omega \rightarrow \omega + \delta\omega_0 \cos\Omega t$, we can compute the phase of the field by integrating once with respect to time

$$\phi(t) = \omega t + \frac{\Omega}{\delta\omega_0} \sin\Omega t = \omega t + \frac{1}{2}\left(\frac{e^{-i\Omega t}}{-i\Omega} + \frac{e^{i\Omega t}}{i\Omega}\right) \tag{1.142}$$

If the frequency perturbation $\delta\omega_0$ is small, we recover a description in terms of a pair of signal sidebands, with amplitudes $\pm\frac{\delta\omega_0}{\Omega}$. This is equivalent to a phase modulation of the field, the only thing changing is the scaling of the physical amplitude of the modulation: there is an additional factor of $1/\Omega$ for frequency noise.

Let's now move on to intensity noise. The simplest way to describe a power fluctuation is to directly modulate the field amplitude at a fixed point in space:

$$E(t) = E_0\left(1 + \frac{1}{2} \cdot \frac{\delta P_0}{P_0} \cos\Omega t\right) \tag{1.143}$$

The factor $1/2$ has been added so that when the modulation is small (which is always the case in our analysis), the power, given by the square of the field, is indeed varying by δP_0. Again, we recognize in the above equation the generation of two signal sidebands, with amplitude proportional to the power fluctuation.

In summary, both intensity and frequency noise can be described by the creation of a pair of signal sidebands around the carrier field, with purely imaginary amplitudes in the case of frequency (or phase) modulation, and purely real amplitudes in the case of intensity noise. Clearly it is enough to study the behavior of the signal sidebands in the power recycled Fabry-Perot-Michelson, and the result is valid for both intensity and frequency or phase noise.

We are now ready to derive the response of the power recycled Fabry-Perot-Michelson interferometer to laser noises, also called *common mode noises*, since the corresponding signal sidebands propagate equally into the two arm cavities. First of all, let's review the response of a simple Fabry-Perot cavity. It is straightforward to write the signal sideband amplitudes into the cavity and in reflection, by generalizing the carrier equations:

$$E_{intra}(\Omega) = \frac{t_i}{1 - r_i r_e e^{2i\frac{\Omega}{c}L}} E_{in}(\Omega) \quad (1.144)$$

$$E_{refl}(\Omega) = \frac{r_i - r_e e^{2i\frac{\Omega}{c}L}}{1 - r_i r_e e^{2i\frac{\Omega}{c}L}} E_{in}(\Omega) = r_{FP}(\Omega)\, E_{in}(\Omega) \quad (1.145)$$

where E_{in} is the field at then input of the Fabry-Perot cavity. For simplicity here we restricted ourselves to the case of a cavity tuned at resonance, and we also neglected the input mirror optical losses. The signal sideband fields inside the cavity show the expected enhancement at low frequency, and the low pass with corner frequency at the cavity poles, similarly to the response to a GW signal (cfr. eq. 1.122). Nothing unexpected here. To compute the response of the power recycled Fabry-Perot-Michelson, we can start by writing the reflectivity of the Fabry-Perot-Michelson, as we have done in sec. 1.5, tuning the Michelson part at dark fringe for the carrier, and taking into account the additional dephasing that the signal sideband accumulates

$$r_M(\Omega) = -e^{2i\frac{\Omega}{c}L} r_{FP}(\Omega) \quad (1.146)$$

From this, we can write an equation similar to eq. 1.135, again taking into account the propagation properties of the signal sidebands:

$$E_{PRC}(\Omega) = \frac{t_p}{1 + r_p r_{FP}(\Omega) e^{2i\frac{\Omega}{c}l_{PRC}}} \quad (1.147)$$

Before diving into this equation, we should realize that the phase accumulated by the signal sidebands into the power recycling cavity is negligible with respect to what is accumulated in the arms. Indeed we have

$$\frac{\Omega}{c} l_{PRC} \simeq \frac{2\pi \times 1000\text{Hz}}{3 \times 10^8 \text{m/s}} \times 100\text{m} \simeq 2 \times 10^{-3} \quad (1.148)$$

Therefore we can neglect everywhere the contribution from the signal propagation over the power recycling cavity length, setting $\frac{\Omega}{c}L \simeq 0$. With this simplification and a bit of algebra we can rewrite the signal sidebands into the power recycling cavity as

$$\begin{aligned} E_{PRC}(\Omega) &= \frac{t_p}{1 + r_p \frac{r_i - r_e e^{2i\frac{\Omega}{c}L}}{1 - r_i r_e e^{2i\frac{\Omega}{c}L}}} \\ &= \frac{t_p(1 - r_i r_e)}{1 + r_i r_p - r_e(r_i + r_p)} \cdot \frac{1 - \frac{r_i r_e}{1 - r_i r_e} 2i\frac{\Omega}{c}L}{1 - \frac{r_e(r_i + r_p)}{1 + r_i r_p - r_e(r_i + r_p)} 2i\frac{\Omega}{c}L} \end{aligned} \tag{1.149}$$

where we used the approximation $e^{2i\frac{\Omega}{c}L} \simeq 1 + 2i\frac{\Omega}{c}L$ as above. Beside from the constant front factor, we can recognize that the frequency dependent part contains two terms. The numerator is a *zero* at the frequency of the cavity pole we already found above. The denominator instead describes a low pass filter, with a corner frequency given by

$$\begin{aligned} \Omega_{PRC} &= \frac{c}{2L} \frac{1 + r_i r_p - r_e(r_i + r_p)}{r_e(r_i + r_p)} \\ &\simeq \frac{c}{2L} \frac{(1 - r_i)(1 - r_p}{2} = \frac{c}{2L} \frac{\pi}{2\mathcal{F}} (1 - r_p) \end{aligned} \tag{1.150}$$

where the approximation is valid for $r_e \simeq 1$ and high reflectivity of both input and power recycling mirrors. The expression above shows that the effect of the power recycling cavity is to move the cavity pole down in frequency by a factor $1 - r_p$. Looking back at eq. 1.149, we can see that any laser noise inside the power recycling cavity is suppressed for frequencies above this *double cavity pole*, until we reach the original Fabry-Perot cavity pole, then the suppression flattens out. But recall that any noise in input of the Fabry-Perot cavity is transmitted to the intra cavity field by means of a low pass at the cavity pole. The combined effect if that any laser noise, by the time it reaches the inside of the Fabry-Perot arm cavities, is suppressed by a single low pass with corner frequency at the double cavity pole.

This is a great advantage, since for the typical values of reflectivities and recycling gains for a second generation detector like Advanced LIGO, the double cavity pole can be at a frequency lower than 1 Hz, providing large suppression of any common mode noise inside the frequency band of interests for the detection of GWs. This effect is crucial in allowing us to relax the very stringent requirements on frequency and intensity noise that we derived for a simple Michelson interferometer.

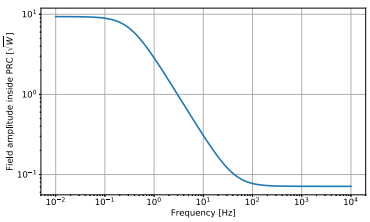

Figure 1.19: Response of the sideband field inside the power recycling cavity to common mode signals.

Before moving on to a new topic, it's useful to gain some physical understand of what's going on and why we get the noise filtering we computed. To build some intuition, let's first start with a single Febry-Perot cavity, and consider a signal sidebands with frequency Ω at the input. If the cavity is at resonance for the carrier, the signal sideband will experience an additional phase shift at each round trip. An equivalent way to think about this is to imagine that the signal sideband is a completely different laser, which is slightly detuned from the cavity resonance. For a over-coupled cavity with reasonably low loss, the reflection when out of resonance is still very close to one, but the phase of the reflected field (the sideband) rotates by an amount which is amplified by the number of round trips in the cavity, with respect to what one would get for free space. So, viewed from the input side, a Fabry-Perot cavity behaves like a high reflectivity mirror, but the phase shift of signal sidebands is larger than a simple mirror by a factor $2\mathcal{F}/\pi$.

Let's now move to the power recycled Fabry-Perot-Michelson interferometer. First of all, we already found that the Michelson-Fabry-Perot can be described as a sort of average of the two arm cavities, when seen from the symmetric port: in other words, when the Michelson part is tuned at dark fringe, the reflectivity as seen from the symmetric port is just the average of the two arm cavities, which for simplicity we take to be equal. Any common mode field at the symmetric input is reflected back, and any differential field (created inside the arms for example) is completely transmitted to the anti-symmetric port. The signal sidebands at the input of the power recycling cavity will therefore see an effective resonant cavity: its input mirror is the power recycling mirror, and its end mirror is constituted of the Fabry-Perot-Michelson interferometer (which is like a mirror with high reflectivity, but amplified phase response). This cavity is at resonance for the carrier, so as the signal frequency increases, the sideband field with move further away from resonance. This will happen quite fast, since the power recycling cavity amplifies any round-trip loss by a number which is roughly proportional to the recycling gain. The round trip phase id dominated by the reflection off the Fabry-Perot cavity, which is already amplified by the cavity round-trip number. Therefore, the signal field phase rotation is amplified twice: first by the arm Fabry-Perot cavity and second by the power recycling cavity. This means that the frequency at which the sideband will start to fall out of the resonance is smaller than both the arm cavity pole and the power recycling pole, resulting in a low pass at the low double cavity pole frequency.

1.7 *Signal recycling*

▷ The power recycled Fabry-Perot-Michelson was the configuration of choice for the first generation of interferometric gravitational wave detectors. The main limitation is the reduced bandwidth of the detectors, due to use of high finesse cavities. In this section we are going to study the last optical trick in our sleeves, which allows us to move the cavity pole up in frequency, recovering a wide band detectors, without sacrificing the peak sensitivity. Magic? No, signal recycling.

The major drawback of using high finesse cavities is that the bandwidth of the detector is reduced: the higher the finesse, the more sensitive the detector is at the peak frequency, but the narrower the frequency response become. The use of power recycling allowed us to effectively increase the laser power, without paying any sensitivity price. Looking at an interferometer diagram, we might recognize that there is still one port where we could add a mirror: the anti-symmetric port. We already discussed above how only differential signal sidebands exit the anti-symmetric port, so it makes sense to call a mirror place there the *signal recycling mirror*. By extension we call the newly formed resonant cavity the *signal recycling cavity*: it is formed by the signal recycling mirror and the Michelson-Fabry-Perot interferometer, as sees from the anti-symmetric port. Since we are going to use both power and signal recycling, we shall call this configuration a *dual recycled Fabry-Perot-Michelson interferometer*.

We've already shown that the Michelson interferometer is highly transmissive, for the signal sidebands coming from the arm cavities toward the anti-symmetric port. To be more precise: if we generate signal sidebands that are of the same amplitude, but opposite sign, in the X and Y arms, they interfere constructively at the beam splitter and are completely transmitted to the anti-symmetric port. With simple symmetry consideration, we can reverse this statement and conclude that any signal sideband inside the signal recycling cavity, that comes back toward the beam splitter, is transmitted differentially to the X and Y arms. In other words, for what concern differential signal sidebands, an interferometer with a signal recycling cavity is effectively a double cavity made of the signal recycling mirror, the arm cavity "average" input mirror and the arm cavity "average" end mirror. This greatly simplify the understanding of signal recycling.

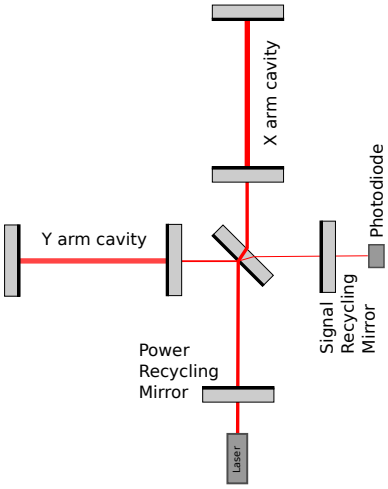

Figure 1.20: A dual recycled Fabry-Perot-Michelson interferometer.

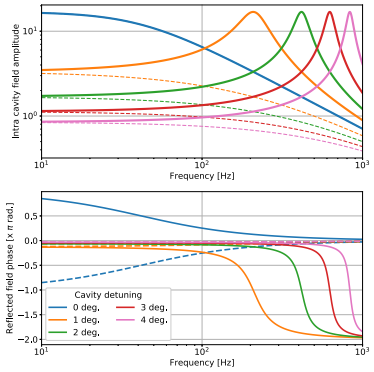

Figure 1.21: Response of a detuned Fabry-Perot cavity. The solid curves show the response of the positive frequency signal sidebands, while the dashed curves show the response of the negative frequency signal sidebands. Results for positive cavity detuning only are shows. Negative detunings produce the same curves, just swapping positive and negative frequency sidebands.

Detuned Fabry-Perot cavity

We will first try to build an intuitive understating of how signal recycling works, and then move on to confirm our understanding with the field equation. But before diving into the signal recycling

business, let's first look back to a simple Fabry-Perot cavity, and see what happens to the signal sidebands when the cavity is not tuned at resonance for the carrier. Let's consider a signal sideband with frequency Ω at the input of *detuned* cavity. If we write for simplicity the phase accumulated by the carrier in a single trip along the cavity as $\phi = kL$, the fields inside the cavity and in reflection are

$$E_{intra}(\Omega) = \frac{t_i}{1 - r_i r_e e^{2i\phi} e^{2i\frac{\Omega}{c}L}} E_{in}(\Omega) \quad (1.151)$$

$$E_{refl}(\Omega) = \frac{r_i - r_e e^{2i\phi} e^{2i\frac{\Omega}{c}L}}{1 - r_i r_e e^{2i\phi} e^{2i\frac{\Omega}{c}L}} E_{in}(\Omega) \quad (1.152)$$

Figure 1.21 shows the effect of a small detuning on the cavity response. First of all, we note that the response for the positive frequency sidebands at $+\Omega$ is different from the response of the negative frequency sidebands at $-\Omega$. This is expected: the cavity is detuned in a definite direction from the resonance (positive for the examples in the figure). The positive frequency sideband (the one that has a time dependency like $e^{i\Omega t}$ and a space dependency like $e^{-i\frac{\Omega}{c}z}$) acquires a negative phase when propagating in the cavity, which for a particular frequency compensates the cavity detuning. Therefore, as visible in fig. 1.21, the intra cavity positive frequency sideband reaches the maximum amplitude at a detuned frequency. The behavior of the negative frequency sideband is opposite: for positive detuning of the cavity they are further away from resonance, and so they are depressed. If we showed the same plot for a negative cavity detuning, the role of negative and positive sidebands would be reversed.

The amplitude of the reflected field is always very close to one, if the optical loss in the cavity is small. But the phase behavior again is different for positive or negative frequency signal sidebands. When the signal sideband frequency crosses the resonance condition in the cavity, we have a fast rotation of the phase of a full 2π. This behavior will play a key role in our understanding of how the signal recycling cavity work.

Signal recycling cavity

When a gravitational wave generates signals in the interferometer, they are in the form of differential signal sidebands: the sidebands generated inside the X arm has the same amplitude but opposite sign than those generated in the Y arm. When these sidebands propagate out of the cavity, toward the corner, they recombine at the beam

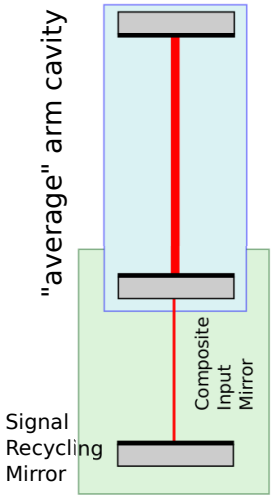

Figure 1.22: A simplified schematic of the signal recycling cavity. Here we consider only the effect on differential signal sidebands. So the Michelson part is not shown, being highly reflective toward the anti-symmetric port. Also the power recycling cavity does not play any role, so it's not shown here. The "average" arm cavity is what is actually seen by the differential sidebands.

splitter constructively, and are transmitted toward the signal recycling cavity. Therefore we can model a signal recycled interferometer as in fig. 1.22: the signal sidebands generated inside the arm do not see simply the arm cavity input mirror, but instead are incident on a composite input mirror, which is the resonant cavity made by the real input mirror and the signal recycling mirror. The properties of this composite mirror depend on the microscopic tuning of the distance between the signal recycling mirror and the input mirror, also called the *signal recycling cavity length*. Depending on the tuning of this cavity $\phi_{SRC} = kl_{SRC} = k\left(l_s + \frac{l_X + l_Y}{2}\right)$ the composite mirror reflection and transmission coefficient are given by the now familiar expressions

$$r(\Omega) = \frac{r_i - r_s e^{2i\phi_{SRC}} e^{2i\frac{\Omega}{c}l_{SRC}}}{1 - r_i r_s e^{2i\phi_{SRC}} e^{2i\frac{\Omega}{c}l_{SRC}}} \tag{1.153}$$

$$t(\Omega) = \frac{t_i t_s e^{i\phi_{SRC}} e^{i\frac{\Omega}{c}l_{SRC}}}{1 - r_i r_s e^{2i\phi_{SRC}} e^{2i\frac{\Omega}{c}l_{SRC}}} \tag{1.154}$$

In second generation interferometers, the signal recycling cavity has a length of few tens of meters, therefore we can ignore the frequency dependent term in the expression above, since $2\frac{\Omega}{c}l_{SRC} \ll 1$, and therefore only the signal recycling tuning matters for determine the behavior of the composite mirror:

$$r(\Omega) = \frac{r_i - r_s e^{2i\phi_{SRC}}}{1 - r_i r_s e^{2i\phi_{SRC}}} \tag{1.155}$$

$$t(\Omega) = \frac{t_i t_s e^{i\phi_{SRC}}}{1 - r_i r_s e^{2i\phi_{SRC}}} \tag{1.156}$$

The behavior of this cavity is a bit different than the over-coupled case we are by now used to. First of all, the signal recycling cavity reflectivity is typically chosen to be smaller than the input mirror reflectivity, and therefore the cavity is under-coupled. Moreover, the signal recycling mirror transmission must be large enough so that we actually get a beam out of the signal recycling cavity, to be detected by a photodiode. In this case, the reflection and transmission of the cavity varies significantly when changing the detuning.

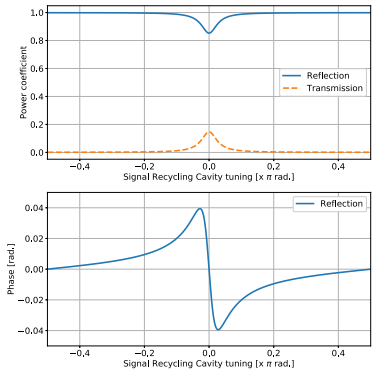

Figure 1.23: Reflection and transmission of the composite input and signal recycling mirror, as a function of the signal recycling cavity tuning.

Resonant signal extraction

Let's first consider the case of $\phi_{SRC} = 0$, meaning that the signal recycling cavity is actually tuned to be resonant for the carrier field (and for low frequency signal sidebands). In this configuration the transmission of the composite mirror is at its largest value, the reflection at its minimum, and the sidebands don't get any additional dephasing in reflection. This implies that the audio sidebands are

propagating inside a cavity (end mirror plus composite mirror) with relatively high transmission, and resonant for the carrier. The low pass frequency for this cavity is larger than the original arm cavity, since the composite mirror reflection is lower. For example, using numbers from Advanced LIGO ($T_i = 1.4\%$ and $T_s = 30\%$), we find that the composite mirror has a transmission of about 15%, instead of the original 1.5% of the input mirror.

$$r_0 = \frac{r_i - r_s}{1 - r_i r_s} \tag{1.157}$$

Therefore the signal sidebands are still low passed, but with a corner frequency that moved up from the original 40 Hz to about 450 Hz. And all this without losing too much of the optical gain enhancement we got from the use of high finesse Fabry-Perot cavities. To see why we don't lose, let's recap how the signals sidebands are generated and how they get to the photodiode:

- The input laser is recycled by the power recycling cavity, and further amplified by the arm cavities, to provide high circulating power in the arm cavities. This is a purely common mode phenomenon, so the presence of the signal recycling cavity does not affect it in any way.

- The GW (or any other differential displacement involving the arm mirrors) creates signal sidebands with amplitude proportional to the field amplitude in the arms, which is roughly proportional to the square root of the recycling gain and the square root of the cavity finesse. So using power recycling and high finesse cavities allow us to produce sidebands with (relatively speaking) large amplitudes. At this stage the sidebands have just been created into the arms, so they have experience anything outside of the arms. Again, having the signal recycling cavity does not change anything.

- Now comes the difference. Without signal recycling, the sidebands are propagating into the same high finesse cavity that generated the power build-up, so before they exit toward the anti-symmetric port, they experience an additional enhancement proportional to the square root of the cavity finesse, but with a low pass filtering effect at the pole frequency of the arm cavity. But, when signal recycling is present, the discussion above shows that the differential sidebands actually propagate into a different cavity, with an equivalent input mirror with much larger transmission, and therefore with largely reduced finesse. They still undergo low passing, but now the corner frequency is at a higher frequency, determined by

the finesse of the composite cavity, which is

$$\mathcal{F}_{\phi_{SRC}=0} = \mathcal{F}_{FP}\frac{1-r_i r_s}{1+r_s} < \mathcal{F}_{FP} \tag{1.158}$$

The factor that multiplies the original cavity finesse $\mathcal{F}_{FP}$ can be made small by choosing the value of the signal recycling mirror reflectivity. For the Advanced LIGO parameters, the finesse is reduced by a factor 0.092, explaining the increase of the cavity pole frequency by a factor of about 10. We have to pay a price for this, that is the sideband amplitude enhancement is lower, since the finesse is lower. But we only lose a factor $\sqrt{10}$ for this example.

In the literature there is quite some confusion about the nomenclature. The correct name of the technique just described, when $\phi_{SRC} = 0$ should be *resonant signal extraction* (RSE) since the signal sidebands are made resonant into the signal recycling cavity, and they are actually extracted more efficiently from the interferometer. Unfortunately, it is common practice to keep calling this configuration *signal recycling*, adding the specification *broad-band signal recycling* to stress the fact that we increased the detector bandwidth, and to distinguish it from the choice $\phi = \frac{\pi}{2}$ that we will discuss below.

Actual signal recycling

What happens if we tune the signal recycling cavity such that the carrier is anti-resonant? This choice would be $\phi_{SRC} = \frac{\pi}{2}$. In this case, the reflectivity of the composite mirror is increased with respect to the original input mirror:

$$r_{\pi/2} = \frac{r_i + r_s}{1 + r_i r_s} \tag{1.159}$$

resulting in a finesse experienced by the sideband which is larger than the original arm cavity:

$$\mathcal{F}_{\pi/2} = \mathcal{F}_{FP}\frac{(1+r_i r_s)}{(1-r_s)} > \mathcal{F}_{FP} \tag{1.160}$$

Therefore in this configuration we further increase the sideband optical gain, but at the price of a much lower cavity pole frequency. So we made the detector bandwidth narrower. For the Advanced LIGO parameters, the finesse increases by more than a factor 10, to a value of about 5000, moving the cavity poles down to about 4 Hz.

This configuration is the one that deserve the proper name *signal recycling*, since in this case the signal sidebands are recycled in a way similar to how the main laser is recycled by the power recycling cavity. However, this tuning is often called *narrow-band signal recycling*, for obvious reasons.

Detuned signal recycling

Finally, what's the effect of choosing any other tuning for the signal recycling cavity $0 < \phi_{SRC} < \frac{\pi}{2}$? Figure 1.23 shows that the reflective of the compound mirror will be somewhere between the two extreme values, as expected. In addition, the phase in reflection changes depending on the tuning of the signal recycling cavity. This will move the carrier field (and the zero frequency signal sidebands) out of resonance. But as we discussed above when we studied a detuned Fabry-Perot cavity, either one of the signal sideband will acquire a dephasing that can compensate this detuning from resonance. Therefore we expect that for a fixed choice of ϕ_{SRC} there will be a frequency where either the positive of negative frequency sideband will be at resonance, and thus enhanced. Therefore the response of the detector will be shaped with a peak at a particular frequency. However, only one of the two signal sidebands will be enhanced at the peak frequency.

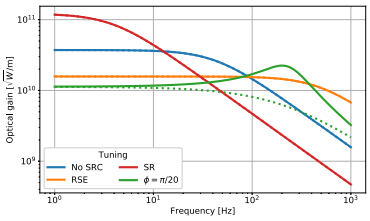

Figure 1.24: Amplitude of the signal sideband fields any the anti-symmetric port in a dual recycled Fabry-Perot-Michelson interferometer with parameters similar to Advanced LIGO and input laser power of 20 W. Solid lines are for negative frequency signal sidebands, while dashed lines are for positive frequency sidebands. For all configuration except the detuned signal recycled case, the response is the same for positive or negative frequency sidebands.

We can put together all the computations done so far, and write in a concise equation the response to a differential arm length change of the signal sidebands at the anti-symmetric port, right on the detection photodiode:

$$\begin{aligned} E_A(\Omega) &= \frac{t_i t_s e^{i\phi_{SRC}}}{1 - r_i r_s e^{2i\phi_{SRC}}} \cdot \frac{1}{1 - r_e e^{2i\frac{\Omega}{c}L} \frac{r_i - r_s e^{2i\phi}}{1 - r_i r_s e^{2i\phi}}} \\ &\quad \cdot 2ik\sqrt{G_{PRC}}\sqrt{\frac{2\mathcal{F}}{\pi}}\frac{\sqrt{P_0}}{2}\, z(\Omega) \end{aligned} \tag{1.161}$$

This equation does not really add much to our understating of how signal recycling works, but we can use it to plot the response of the fields impinging on the photodetectors as a function of the signal frequency and the signal recycling cavity tuning, see fig. 1.24. The figure compares the response of a detector without signal recycling, to the response of a dual recycled interferometer, with different tunings of the signal recycling cavity. What is plotted there is the response of the signal sideband fields as a function of frequency. For all configurations, except the detuned case, the response of the two signal sideband is equal. For the detuned case, as anticipated, only one of the two sideband gets a resonant improvement.

The additional factor $\frac{1}{2}$ comes from the splitting of the displacement into the two signal sidebands $z(t) = z_0 \cos\Omega t = \frac{z_0}{2}\left(e^{i\Omega t} + e^{-i\Omega t}\right)$.

1.8 Summary

In this chapter we built the basics tool needed to describe how a interferometer respond to a gravitational wave signal. We also dis-

cussed the basic limitation to the sensitivity, which is the shot noise due to the quantum nature of light. Starting from a simple Michelson interferometer, we added more and more complexity, with the goal of increasing as much as possible the detector sensitivity. Figure 1.25 shows the shot-noise-limited sensitivities for the configuration we described. The first generation of interferometric detectors were Power Recycled Michelson Interferometers with Fabry-Perot cavities. The finesse was as low as 50 (Virgo) and up to 150(Virgo+) and 200 (iLIGO and eLIGO). The second generation of detectors (Advanced LIGO) that discovered gravitational waves are Dual Recycled Michelson interferometers with Fabry-Perot cavities, operated in the resonant signal extraction configuration. This choice allowed a larger bandwidth, paying a small price in terms of peak sensitivity. We will see in chapter **??** that the advanced detector sensitivity is not limited by shot noise at frequencies below 100 Hz, so the increased low frequency shot noise due to the RSE configuration is not so important.

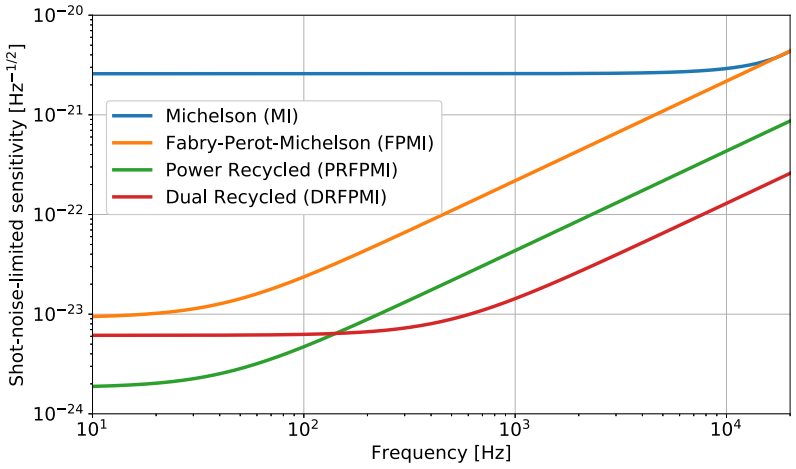

Figure 1.25: Comparison of the shot-noise-limited sensitivity of all the configurations described in this chapter. The parameters used are arm length $L = 4$ km, Fabry-Perot finesse $\mathcal{F} = 450$, arm cavity round trip loss $L = 75$ ppm, power recycling mirror transmission $R_p = 3\%$, signal recycling mirror transmission $T_s = 35\%$, input power $P_i = 25$ W.